SC/66b/IA/08

# Simulation studies on the properties of estimates from statistical catch at age models

William de la Mare

INTERNATIONAL
WHALING COMMISSION

# Simulation studies on the properties of estimates from statistical catch at age models.

William K. de la Mare.
Australian Antarctic Division, Channel Highway, Kingston, Tasmania, Australia, 7050.

**Abstract**
An age-structured population dynamics model is used to generate simulated data on abundance and catch-at-age at times and with sample sizes approximately corresponding to the data available for Southern Hemisphere minke whales. A model from the same family is fitted to these data using the methods of statistical catch at age analysis (SCAA). The results show that estimates have rather poor properties and are quite uninformative about maximum sustainable yield rate (MSYR) and at best only weakly informative about any trends in carrying capacity (*K*). The results suggest that the historical contrast in the data is relatively uninformative about the management parameters of interest. The more recent and future data are from a period when even less contrast in population characteristics exists or can be expected. For this reason the recent data are not informative about trends in *K* or MSYR and the collection of further data has little effect on improving precision of such estimates.

## Introduction

Statistical catch at age analysis models (SCAA) have become a mainstay of a number of analyses seeking to estimate a range of parameters of management interest by fitting population models to a range of data types, typically combining catch-at-age data with time series of abundance data. The important developments in this space have been driven by Punt and Polacheck (2005. 2006, 2007 and 2008) and in a series of update and model improvements (Punt; 2011, Punt et al. 2014). Much of this development was originally to address the issue of whether catch-at-age data from southern hemisphere minke whales carried a signature of population trends that pre-date their exploitation and that may have arisen from the depletion of other baleen whales – particularly blue whales earlier last century; the much discussed 'krill surplus'. This question was addressed by using SCAA models to fit population models that allow for changes in carrying capacity (*K*) over time. SCAA models generally need to estimate tens to hundreds of parameters and to be computationally tractable they rely on maximisation of log-likelihood functions by numerical methods that make use of auto-differentiation.

These models are beginning to be relied upon to utilise the catch-age-data from JARPA, JARPAII and NEWREP-A to meet those programs' objectives of providing information relevant to management and the development of ecosystem models. Therefore it is timely to use simulation methods to improve our knowledge of the reliability of estimates arising from these models and to develop methods for the prospective evaluation of the likely outcomes from collecting further abundance and age-data.

A second issue is that if the models are to be used for the derivation of management related information, the SC should follow its normal practice and have them independently validated. The model presented here has been developed independently and makes no use of any code used in the existing SCAAA model. Consequently inter-comparison of the two model implementations using simulated data could be used to assist in their validation.

The model used in the simulations here is built using an object oriented class template library written in C++ originally developed for stock-assessment and management strategy evaluations (Logan *et al.* 2005). The class template models can be instantiated with variables declared as double precision or as auto-differentiable while using identical source code for model implementation. This readily allows for multiple instances of the model so that for simulation testing it is easy to set up one instance of the model for data generation and an entirely independent instance to be used for fitting to data. The details of the model are given in the Appendix.

The fitted model uses an auto-differentiation class template library developed by Justin Cooke. Testing showed that the fitted model with auto-differentiation produces identical numerical results to the data-generating simulation model when the same parameter values are used. The fitting procedure recovers the 'true' values of the data generating model parameters when fitted using perfect information. Although the model presented here has the sexes pooled, the class library also contains two sex versions of the model and so the model can be readily extended. However, for the purposes of this paper which is to begin to define the issues relevant for SCAA modelling, a pooled sex model is sufficient.

The model presented here provides for more flexible estimation of some of the relationships included in the existing SCAA models. In particular Punt *et al.* (2014) used piece-wise linear functions to describe changes in *K* and the shape of age-dependent natural mortality as well as a discontinuous function for 'dome shaped' commercial age-specific catch selectivity. The difficulty with piece-wise linear and other discontinuous functions is that they do not have continuous derivatives at the joints, which makes it difficult to estimate the position of the joints using auto-differentiation. The positions of the joints are not included in the estimation procedure in the existing SCAA models.

In the models used in this study that time variations in *K* are modelled using a dome-shaped curve derived from multiplying a logistic function with a reversed logistic function. This combined function has continuous differentials (see Appendix for definition). The same functional form is used for dome-shaped selectivities. Age dependence in natural mortality is modelled using a continuous function of the general form due to Siler (1979), but with an additional parameter to defer increasing mortality with age (see Appendix). Here, as in the existing SCAA the value of MSYL is kept fixed.

A more subtle difficulty arises in the existing SCAA and other models that use a Pella-Tomlinson (P-T) stock-recruitment relationship. With a P-T model, population levels somewhat above *K* lead to negative

recruitment. The existing SCAA includes the usual practice of resetting negative recruitment values to zero and penalising the likelihood function. However, this also destroys the continuity of the function. In the models presented here all of the functions to be fitted, including the stock-recruitment relationship, are continuous and so estimating all of their parameters is feasible when using auto-differentiation. The population dynamics model, the functional forms for model components and other variable functions and the likelihood functions used in fitting are all given in the Appendix.

The scenarios tested here are based on plausible hypotheses relating to southern hemisphere minke whales and the types of data collected under JARPA, JARPA II and prospectively under NEWREP-A. These initial tests are idealised because all animals in the catch are aged without error and the catch-at-age distributions represent random samples from the selected population. Age-specific selectivities are also constant over time for both commercial and special permit catches. There are two series of absolute abundance estimates, one corresponding to the IDCR/SOWER surveys (generously assuming that there were three comparable surveys) and the second to the JARPA, JARPA II and prospectively NEWREP-A at two year intervals. Neither series is assumed to be unbiased, each has its own correction factor estimated during minimisation as a time-invariant constant.

All the simulated data conform to the assumptions used in fitting the model. Consequently the performance of the estimation procedure is evaluated under ideal circumstances. The list of all the estimated parameters is given in Table 1. However, recruitment multipliers are not estimated in scenarios where there is no variability in $K$, thus correctly assuming that there is negligible recruitment variability. The numerical search makes two passes, the first initialises the nuisance harvest rate parameters into roughly the correct starting values. There are multiple restarts for the search with randomly dithered starting values for the parameters, centred in these trials on their true values, with increasing stringency for the convergence criteria. This is to reduce the possibility of landing on a local minimum. This is particularly important for multiple replicates in simulation testing because it is not feasible to examine the fit of every estimate in the same way as one would do for fitting a model to a single dataset. With complex multi-parameter likelihood functions it is likely that the morphology of the surface may exhibit local minima or twisting valleys, both of which make it possible for searches to converge even though there is a different set of parameter values that have a better minimum.

*Table 1. Parameters estimated during fitting of model to simulated data. The searches for parameters are all constrained to a range by using a logit function to transform the parameters. In this way the transformed parameters are unbounded during the numerical search, but after the inverse transform the estimated values will lie in the bounded region. The column Order refers to the order in which the parameters are estimated in the fitting procedure. Generally the harvest rate nuisance parameters and stock size are estimated first with the other parameters held at their starting values. After the first pass all the parameters are estimated together. This is more efficient because it gives the nuisance parameters roughly correct values before searching over the entire parameter space.*

| **Parameter** | **Lower bound** | **Upper bound** | **Order** |
|---|---|---|---|
| Initial total biomass (tonnes) | 200 000 | 1 600 000 | 1 |
| Stock recruit compensation | 2.001 | 5.0 | 2 |
| Density dependence in natural mortality | 0.0 | 1.0 | 2 |
| Siler coefficient 1 | 0.03 | 0.2 | 2 |
| Siler coefficient 2 | 0.5 | 4.0 | 2 |
| Siler coefficient 3 (floor on M) | 0.02 | 0.12 | 2 |
| Siler coefficient 4 | 0.1 | 0.5 | 2 |
| Siler coefficient 5 | 40 | 65 | 2 |
| Peak value for difference in $K$ (as multiple of $K$) | -0.8 | 5.0 | 2 |
| First inflection year for $K$ scaling | 1930 | 1955 | 2 |
| Number of years to first 95% point on $K$ scaling | 0. | 10. | 2 |
| Extra years to second 95% point on $K$ scaling | 1. | 30. | 2 |
| Extra years to second inflection for $K$ scaling | 1. | 30. | 2 |
| First inflection for commercial age selectivity | 1 | 12 | 2 |
| Additional age to lower 95% commercial age selectivity | 1 | 12 | 2 |
| Additional age to upper 95% commercial age selectivity | 1 | 40 | 2 |
| Additional age to second inflection commercial selectivity | 1 | 20 | 2 |
| Inflection for special permit age selectivity | 0.2 | 4.0 | 2 |
| Additional age for 95% point for special permit selectivity | 0.2 | 5.0 | 2 |
| Survey bias for IDCR/SOWER | 0.5 | 5.0 | 2 |
| Survey bias for special permit surveys | 0.2 | 5.0 | 2 |
| Harvest rates (for every year with a non-zero catch | 0. | 0.1 | 1 |
| Year class multipliers (from 1940 – 2004) | 0.1 | 2. | 2 |

The basic test scenarios examine different historical patterns of changes in carrying capacity and different strengths of density dependence in relation to natural mortality and births. A further set of scenarios examine the effect of adding additional years of age-data (every year) and surveys every two years. In these latter scenarios the amount of data available is probably greater than will occur in practice.

**Test 1 – *K* increases and then declines, with variability = 0.3 – all density dependence is in births**
This scenario is roughly similar to the "base case" reported in Punt *et al.* (2014.) Minimisation in each trial either starts from a low MSYR = 1% or a high MSYR = 5%. The true MSYR = 3.64%. As will be demonstrated across all the scenarios, there is little information about MSYR from the data available for Southern hemisphere minke whales. This is consistent with the results of Punt *et al*. that the estimates of MSYR are not reliable. As will be seen the estimates of MSYR are influenced by the starting values used in the search. So results will be shown for high and low MSYR starts for all scenarios.

Summary statistics of the results are shown in Table 2. The most important feature to note is the effect of the starting point for MSYR on the results. The estimated values of MSYR are biased high or low depending on the starting point and thus the coefficients of variation do not represent the full uncertainty in the estimates. The estimates of delta *K* are also biased although they are more consistent between the high and low MSYR starting points.

Fig 1 shows the observed and expected total catches are very close – these plots are virtually identical in every test scenario and so this figure will not be shown again. Similarly for Figs 3 and 4 the fits to the two sources of catch-at-age data are very close and this is also consistent across scenarios. These plots will only be shown again in the first scenario where density dependence acts on both births and natural mortality. Fig 6 shows the fit to the two types of survey data. These results are also comparable across all scenarios and this figure will also be omitted hereafter.

Figs 5 and 9 show that the trend in *K* is poorly estimated, but they are consistent in that all of the estimated values of delta *K* are positive. Figs 6, 7, 8 and Figs 9, 10 and 11 show that there can be substantial biases in estimating trends in recruitment and that these biases are different for the high and low MSYR starts. The lower two sections of Table 2 show that although the marginal likelihoods for MSYR and delta *K* are fairly flat, there is an indication that the data and model in this scenario provide some discrimination against the lowest MSYR tested and delta *K* = 0.

Figs 8 and 11 show that there are trends in the estimates of the means of the recruitment multipliers and these depart substantially from the theoretical mean of unity. This indicates that the recruitment multipliers are absorbing some lack of fit in the model arising from the stock recruitment relationship.

*Table 2. Properties of estimates from Test 1. The first sub-table are the estimates of MSYR and Delta K from 100 trials. The second sub-table is the mean marginal total negative log-likelihood profiles from 25 replicates with identical data for each fixed value of Delta K, and also subdivided for the different data sources. The third sub-table is the mean marginal total negative log-likelihood profiles from 25 replicates with identical data for each fixed value of MSYR, and also subdivided for the different data sources.*

| Start | MSYR estimates (true = 0.0364) | | | | Delta *K* estimates (true = 2.0) | | | |
|---|---|---|---|---|---|---|---|---|
| | Mean | SD | CV | Bias | Mean | SD | CV | Bias |
| High | 0.048 | 0.0102 | 0.210 | 1.330 | 2.16 | 0.629 | 0.291 | 1.082 |
| Low | 0.019 | 0.0039 | 0.208 | 0.522 | 2.36 | 0.712 | 0.302 | 1.179 |

| Delta K | Total | Survey 1 | Survey 2 | Comm. Ages | S. permit Ages |
|---|---|---|---|---|---|
| 0.0 | 4374.536 | 35.06530 | 125.6548 | 1734.667 | 2224.925 |
| 1.0 | 4370.670 | 35.05068 | 125.3368 | 1731.878 | 2224.555 |
| 2.0 | 4369.641 | 35.05427 | 124.9275 | 1734.423 | 2221.915 |
| 3.0 | 4370.946 | 35.25407 | 125.4597 | 1734.064 | 2221.679 |
| 4.0 | 4368.948 | 35.42701 | 125.2958 | 1733.000 | 2220.737 |

| MSYR | Total | Survey 1 | Survey 2 | Comm. Ages | S. permit Ages |
|---|---|---|---|---|---|
| 0.01 | 4385.431 | 35.07727 | 125.2926 | 1739.193 | 2231.972 |
| 0.02 | 4377.205 | 35.05811 | 125.3936 | 1736.063 | 2226.812 |
| 0.03 | 4377.815 | 35.04081 | 125.3418 | 1736.279 | 2227.334 |
| 0.04 | 4378.595 | 35.03605 | 125.3981 | 1736.242 | 2228.040 |
| 0.05 | 4378.760 | 35.08902 | 125.6623 | 1736.013 | 2227.864 |

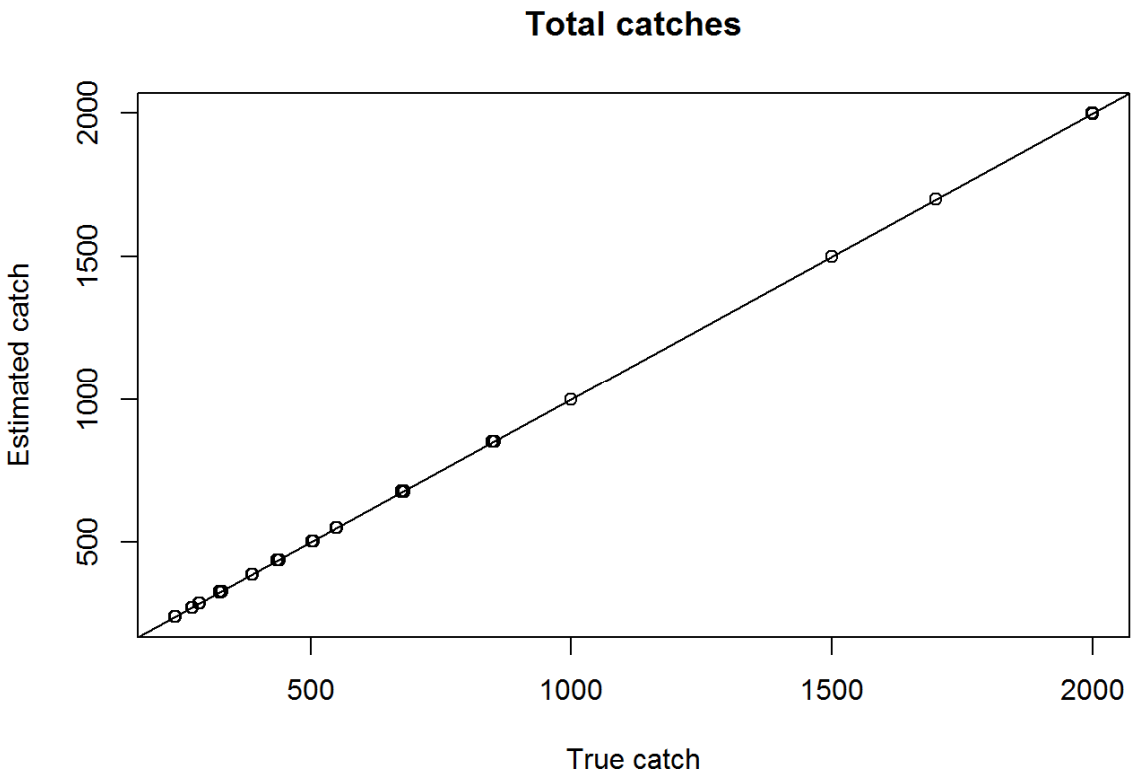


Fig 1 Comparison of observed and expected catches from high MSYR fit of model in Test scenario 1

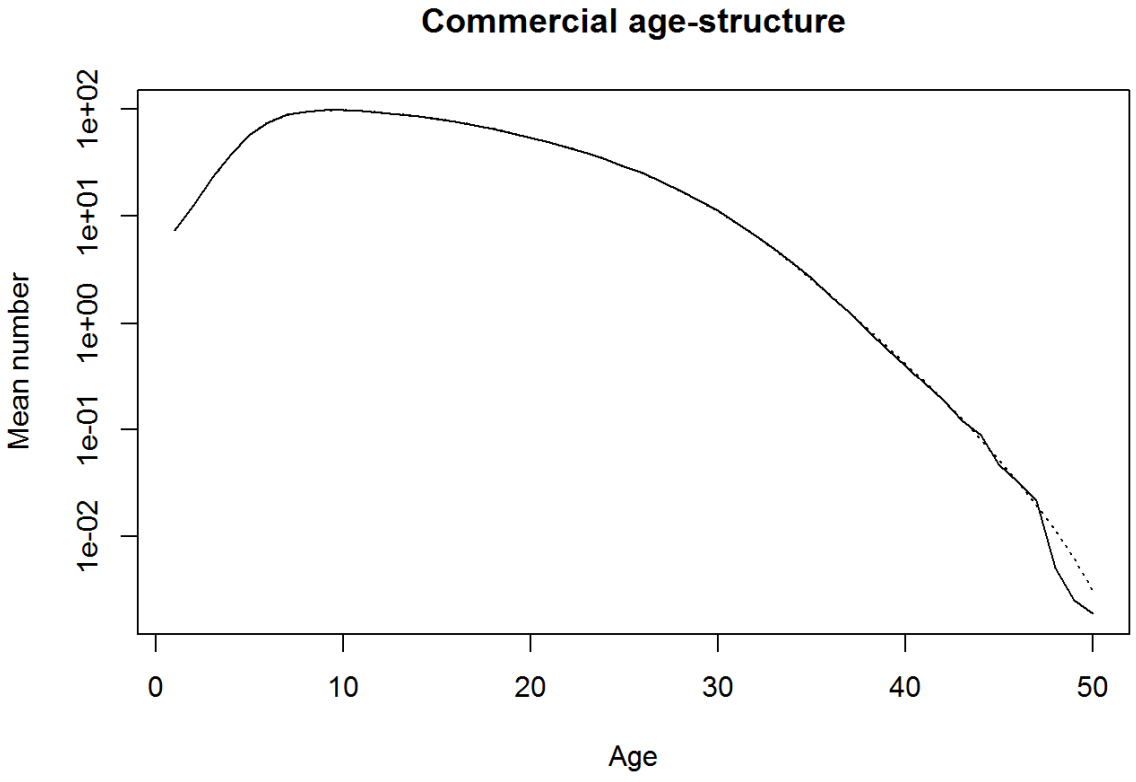


Fig 2. Mean of the expected commercial catches-at-age high MSYR fit of model (dashed line) compared with the true mean catch-at-age (solid line) from Test scenario 1.


Fig 3. Mean of the special permit expected catches-at-age from high MSYR fit of model (dashed line) compared with the true mean catch-at-age (solid line) from Test scenario 1

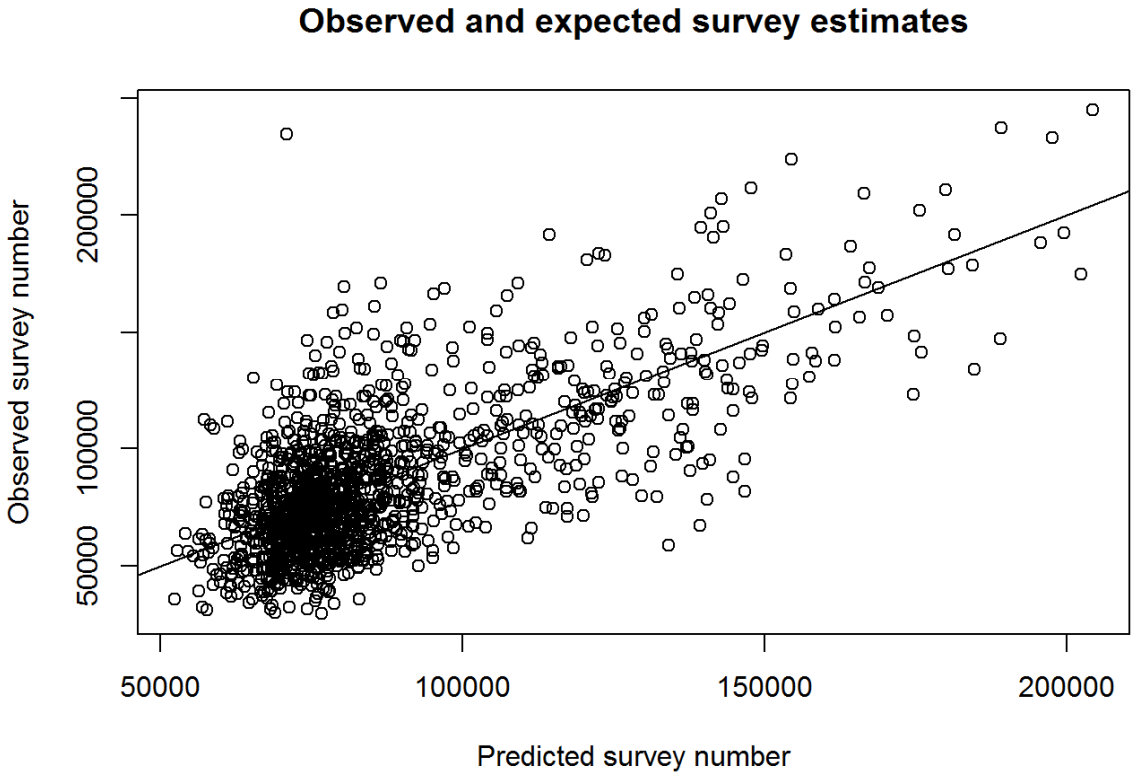


Fig 4. Observed and expected survey results from high MSYR fit of model replicates in Test scenario 1.

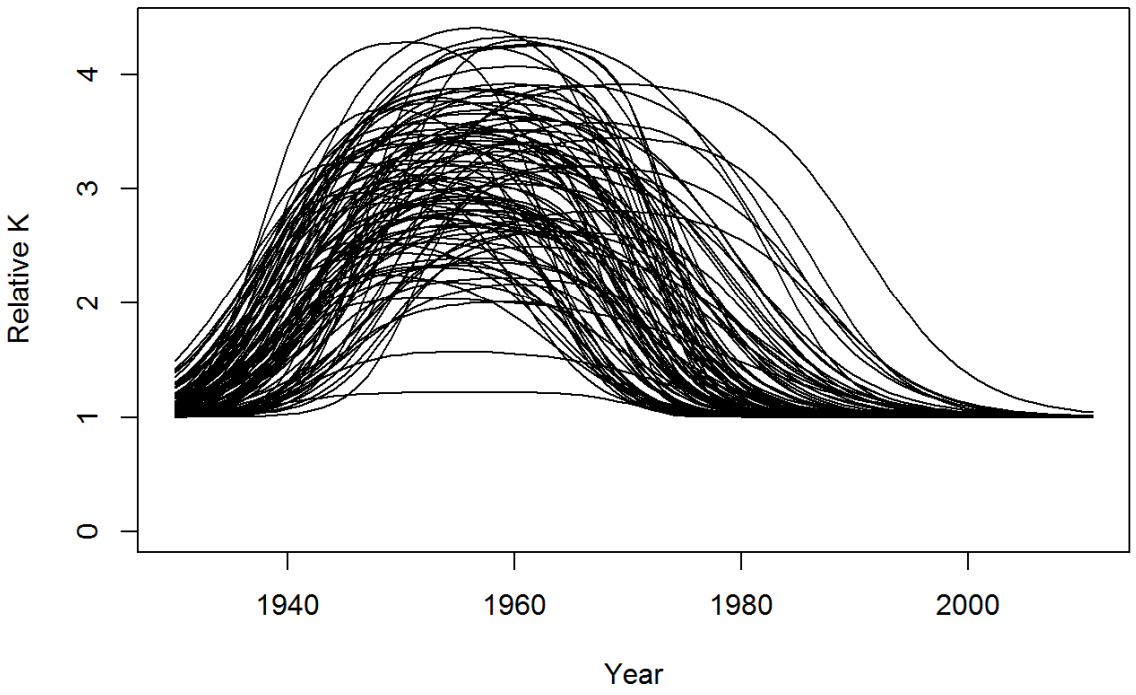


Fig 5. The trends in *K* from high MSYR fit of model for Test Scenario 1.

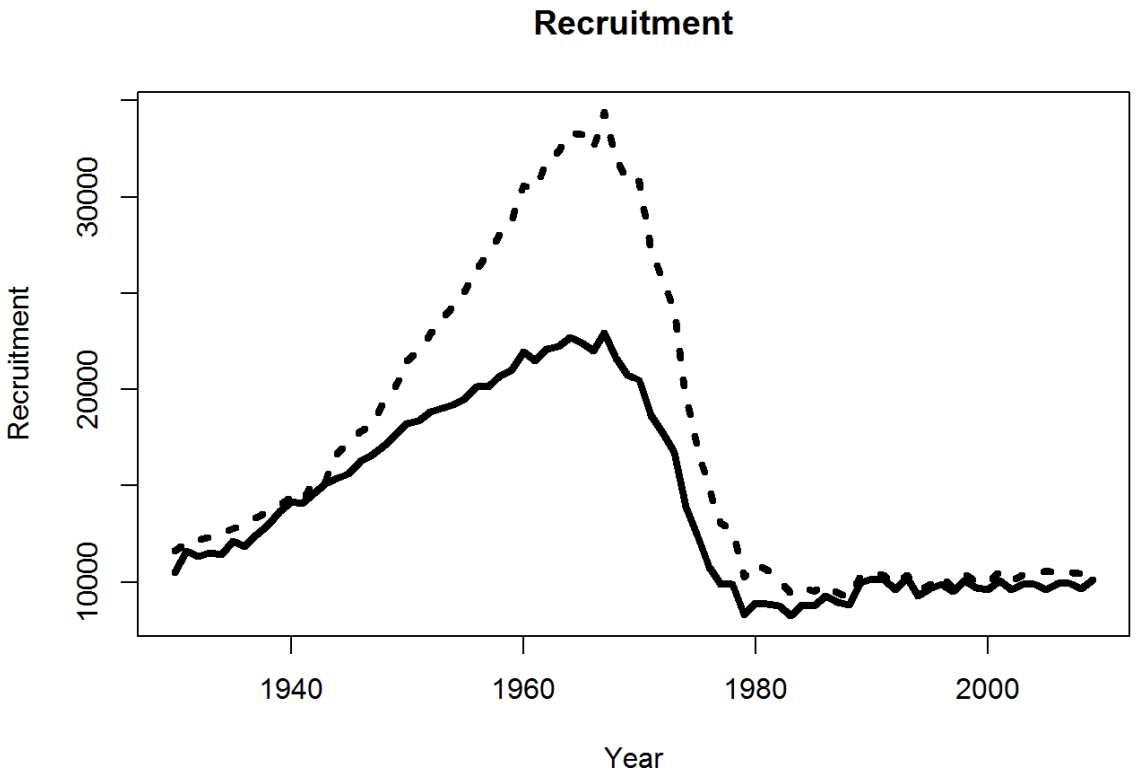


Fig 6. The mean estimated recruitment trajectory (dashed line) from the high MSYR fit of model compared with mean true trajectory for Test scenario 1.

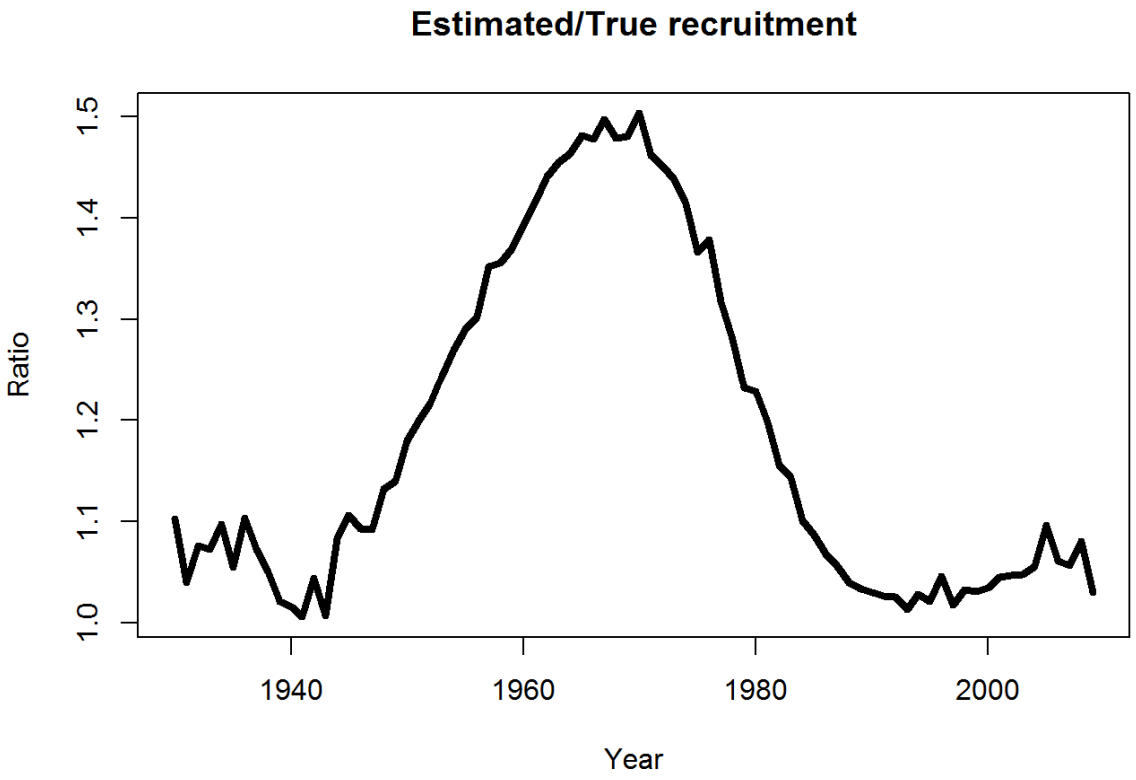


Fig 7. The estimated bias in recruitment from high MSYR fit of model under Test Scenario 1.

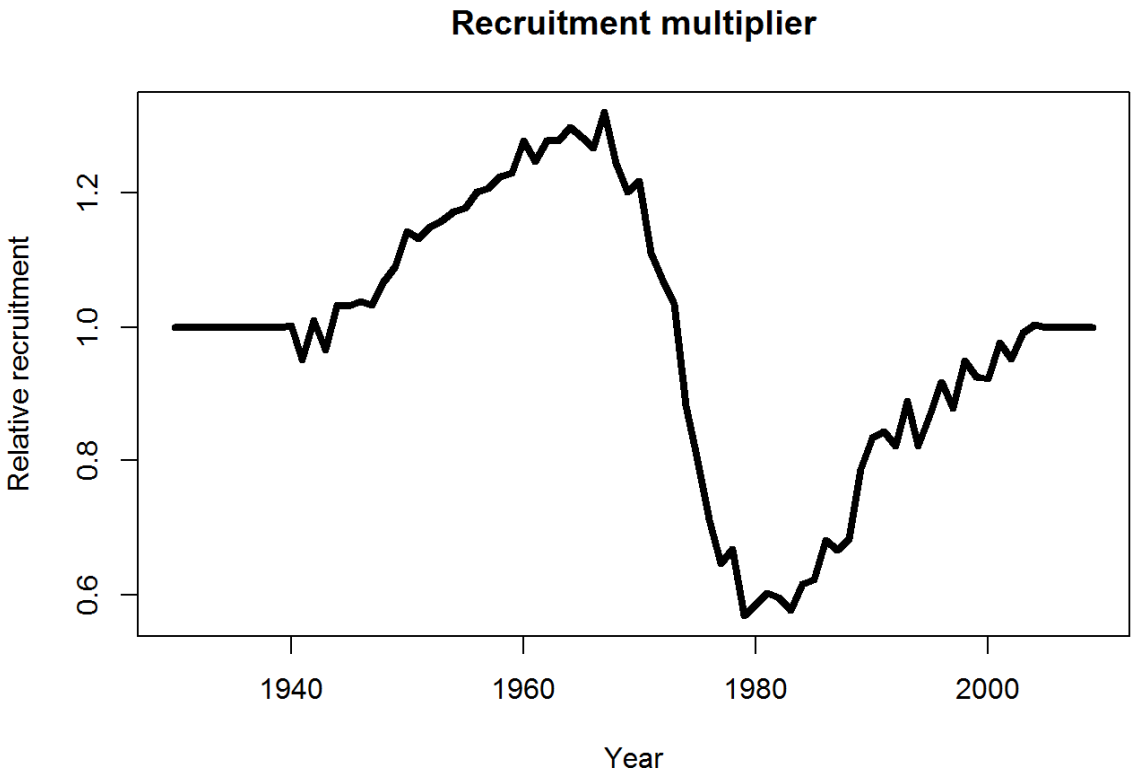


Fig 8. The means of the recruitment multiplier estimates from high MSYR fit of model under Test scenario 1.

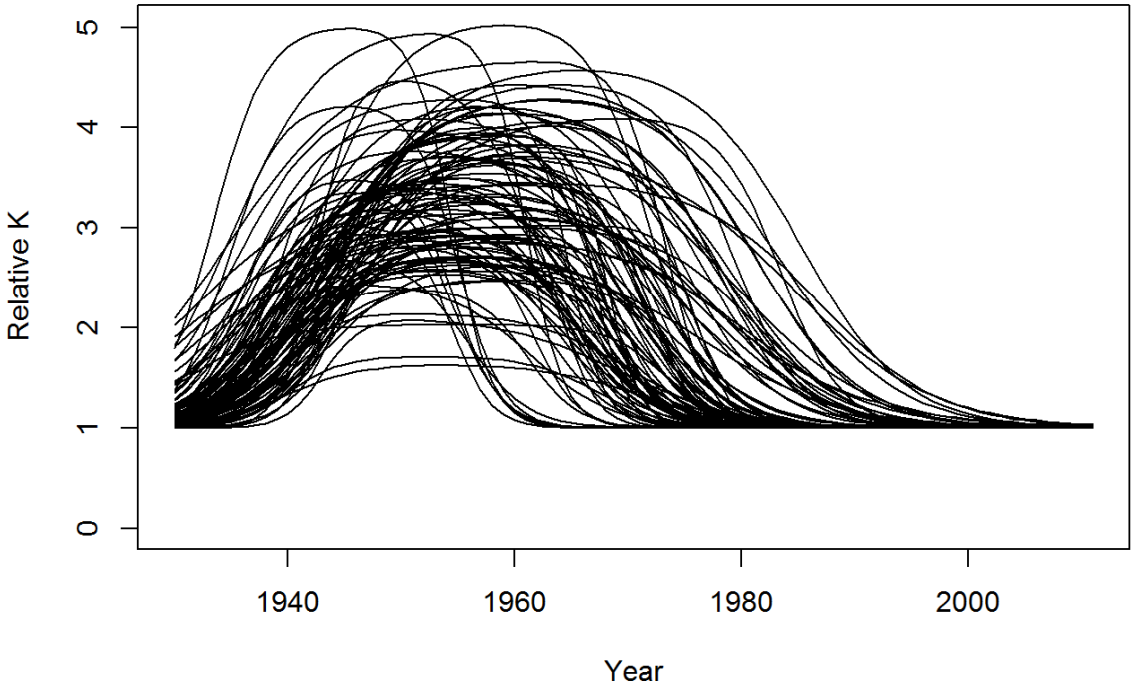


Fig 9. The trends in *K* from low MSYR fit of model for Test Scenario 1.


Fig 10. The estimated bias in recruitment from low MSYR fit of model under Test Scenario 1.

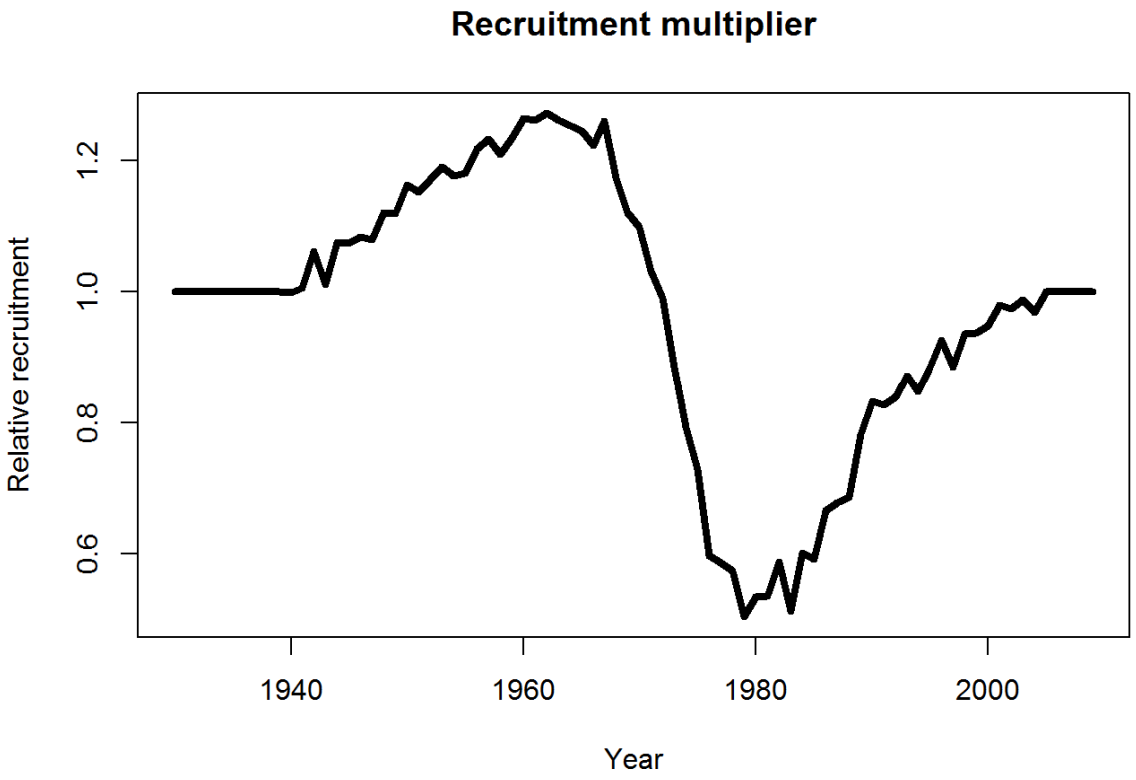


Fig 11. The means of the recruitment multiplier estimates from low MSYR fit of model under Test scenario 1.

**Test 2 *K* increases and then declines with variability = 0.3 – all density dependence is in births – data extended to 2027**

This is the same as Test 1 but with data extended to 2027 with catch-at-age in every year with a sample size of 330 and surveys every second year. This is more age data than is projected to be collected in a single sector under NEWREP-A. The main claim for SCAA in relation to NEWREP-A is that more years of age data will improve estimates from the method. Comparing tables 2 and 3 show that there the overall statistics for MSYR and delta *K* are virtually unchanged despite the extra years of data. Figs 12 and 15 with Figs 5 and 9 show that there has been no discernable improvements in the estimates of time trends in *K*. The patterns and magnitudes of bias in the estimates of recruitment also show little change (Figs 13 and 16 with Figs 7 and 10). The trends in the recruitment multipliers also are little changed. This is not surprising because these trends are primarily driven by the historical commercial catch-at-age data, which of course remains the same between Tests 1 and 2.

*Table 3 shows the results from 100 replicates from both the high and low MSYR starts. Comparing these results with the corresponding rows in Table 2 shows that there is negligible improvement in the estimates of MSYR and delta K with the addition of more years of data. Figures 12 through 17 show that there are negligible improvements in the estimation of relative recruitment and recruitment multipliers with the extra years of data.*

| Start | MSYR estimates (true = 0.0364) | | | | Delta *K* estimates (true = 2.0) | | | |
|---|---|---|---|---|---|---|---|---|
| | Mean | SD | CV | Bias | Mean | SD | CV | Bias |
| High | 0.049 | 0.0098 | 0.199 | 1.353 | 2.27 | 0.656 | 0.288 | 1.137 |
| Low | 0.019 | 0.0043 | 0.231 | 0.508 | 2.37 | 0.685 | 0.289 | 1.184 |

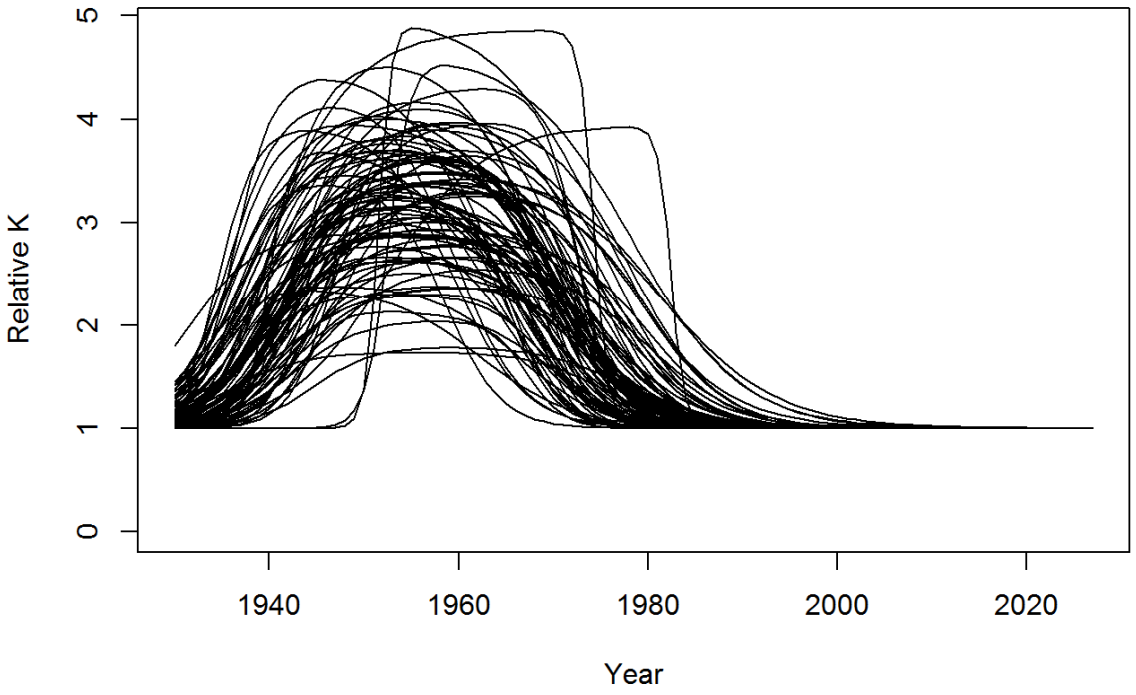


Fig 12. The trends in *K* from high MSYR fit of model for Test Scenario 2.

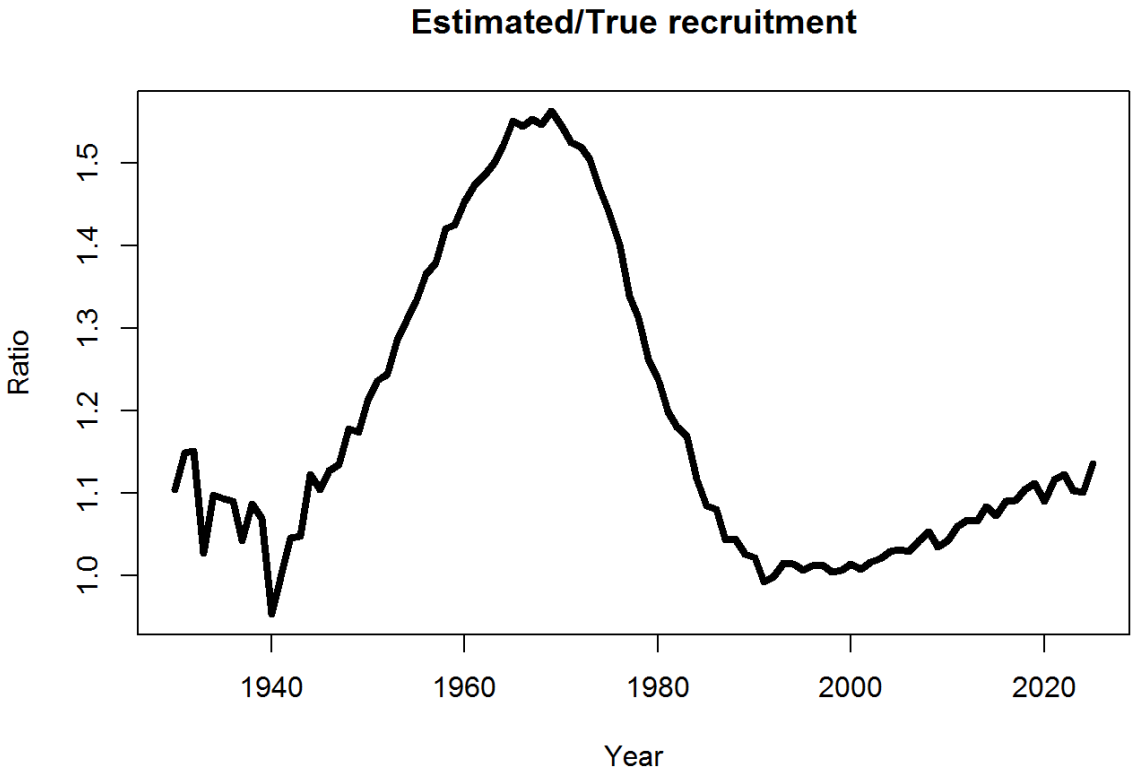


Fig 13. The estimated bias in recruitment from high MSYR fit of model under Test Scenario 2.

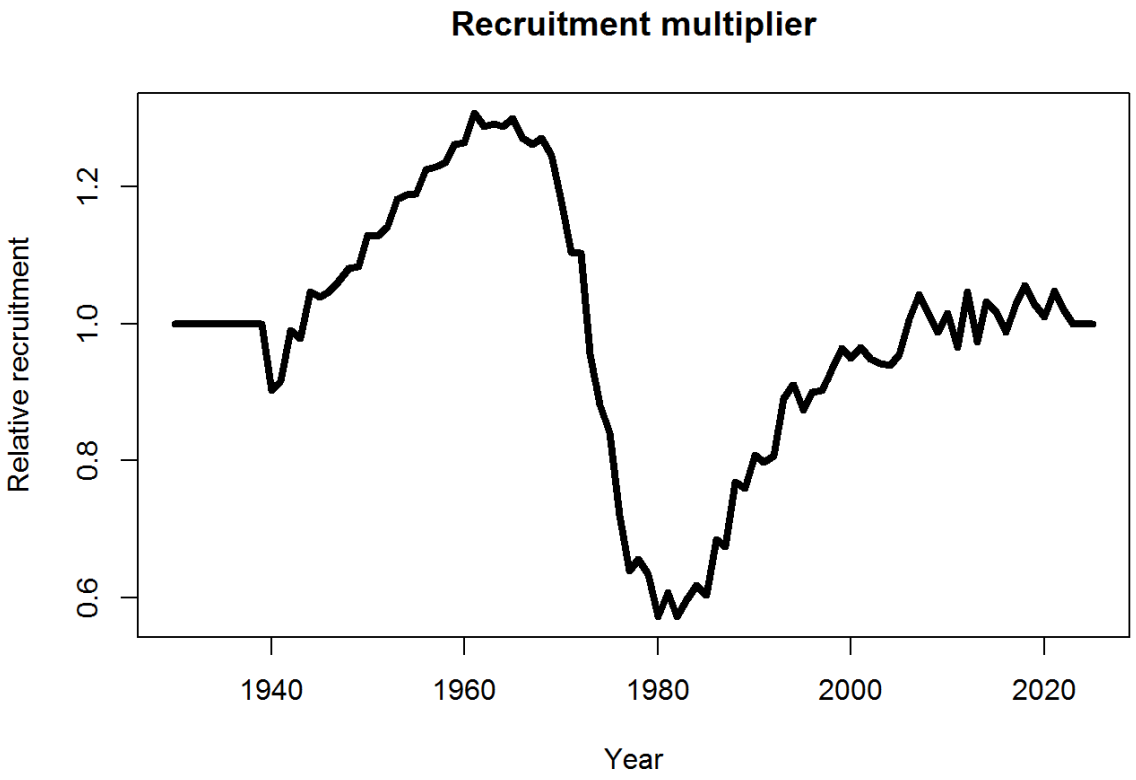


Fig 14. The means of the recruitment multiplier estimates from high MSYR fit of model under Test scenario 2.

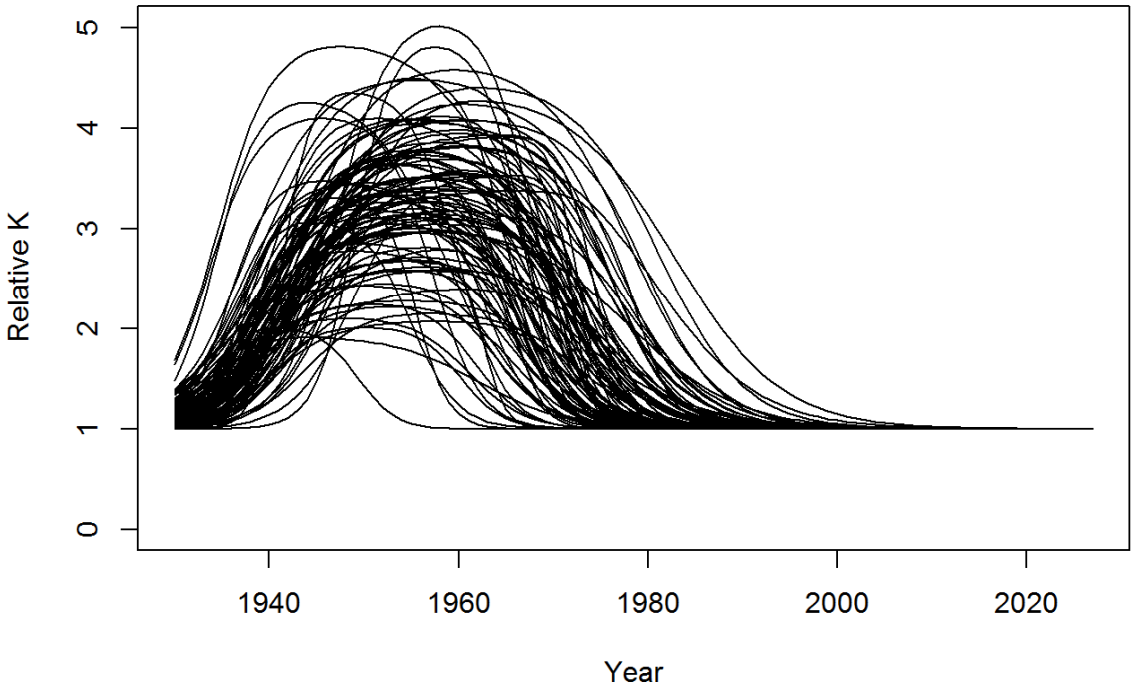


Fig 15. The trends in *K* from low MSYR fit of model for Test Scenario 2.

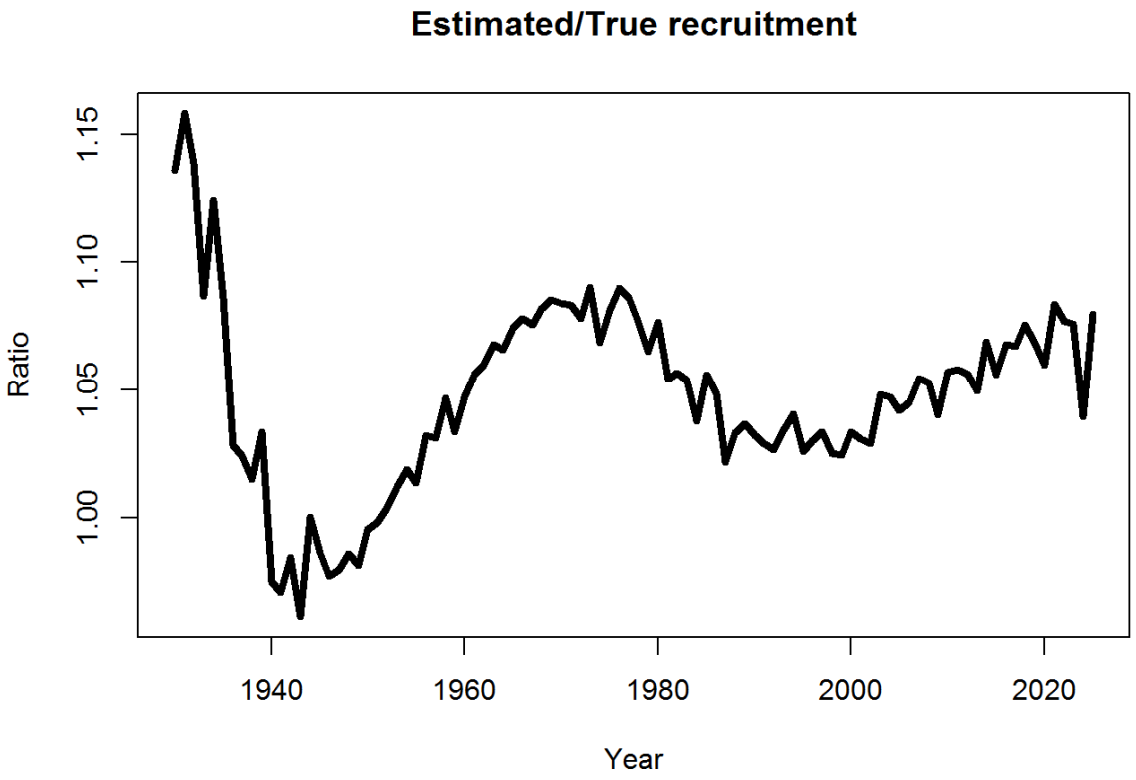


Fig 16. The estimated bias in recruitment from low MSYR fit of model under Test Scenario 2.

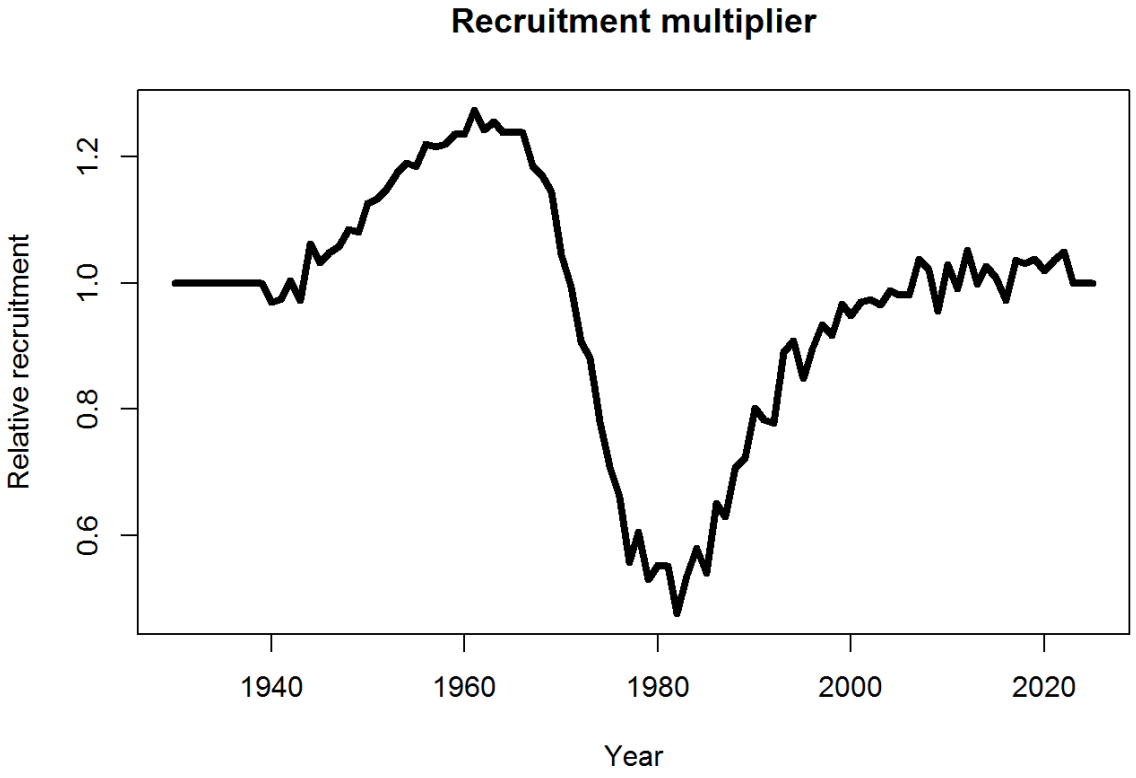


Fig 17. The means of the recruitment multiplier estimates from low MSYR fit of model under Test scenario 2.

**Test 3 *K* increases and then declines with variability = 0.0 – density dependence is 75% in natural mortality and 25% in births**

In this scenario density dependence in natural mortality is substantially greater than it is for births. This is consistent with the emergent properties of the energetics based models reported in de la Mare and Miller (this meeting). One of the consequences of this form of density dependence is that the signature of a trend in carrying capacity is different from that obtained when all density dependence occurs in births. This is easily seen by comparing Figs 3 and 19. Fig 3 shows a distinct bump caused by the set of stronger year classes arising from the trend in *K*. However in Fig 19 the bump is virtually absent because the variation in year class strength is much less, and the density dependent variation in natural mortality affects all the year classes together so that there is a smaller transient effect on the age-structure.

Table 4 shows that the estimates of MSYR have roughly the same statistics as for Test 1, with similar bias dependency on the starting values and similar coefficients of variation. However, the estimates of delta *K* are substantially different, with this scenario Figs 20 and 23 show that not all the estimates of delta *K* are positive, which leads to substantial downward bias in the estimates and consequently greater CVs. Figs 21 and 24 show that the estimates of recruitment are of the correct general shape but Figs 22 and 25 show a time varying bias of 25 to 35%. Recruitment multipliers are not estimated in this case because they are correctly assumed to be all equal to unity. The marginal likelihoods in Table 4 for delta *K* and MSYR again suggest that there is some discrimination for the lowest values.

*Table 4. Properties of estimates from Test 3. The first sub-table are the estimates of MSYR and Delta K from 100 trials. The second sub-table is the mean marginal total negative log-likelihood profiles from 25 replicates with identical data for each fixed value of Delta K, and also subdivided for the different data sources. The third sub-table is the mean marginal total negative log-likelihood profiles from 25 replicates with identical data for each fixed value of MSYR, and also subdivided for the different data sources.*

| Start | MSYR estimates (true = 0.0364) | | | | Delta *K* estimates (true = 2.0) | | | |
|---|---|---|---|---|---|---|---|---|
| | Mean | SD | CV | Bias | Mean | SD | CV | Bias |
| High | 0.045 | 0.0099 | 0.221 | 1.222 | 0.843 | 0.682 | 0.808 | 0.422 |
| Low | 0.019 | 0.0078 | 0.404 | 0.527 | 0.907 | 0.701 | 0.773 | 0.453 |

| Delta K | Total | Survey 1 | Survey 2 | Comm. Ages | S. permit Ages |
|---|---|---|---|---|---|
| 0.0 | 4363.798 | 35.60212 | 127.0312 | 1791.733 | 2152.299 |
| 1.0 | 4351.236 | 35.49600 | 126.9508 | 1781.513 | 2150.478 |
| 2.0 | 4351.268 | 35.51740 | 126.9786 | 1781.411 | 2150.478 |
| 3.0 | 4350.620 | 35.55955 | 127.0513 | 1780.998 | 2150.036 |
| 4.0 | 4350.462 | 35.52077 | 127.0990 | 1782.080 | 2149.031 |

| MSYR | Total | Survey 1 | Survey 2 | Comm. Ages | S. permit Ages |
|---|---|---|---|---|---|
| 0.01 | 4362.278 | 35.62042 | 126.9568 | 1790.608 | 2151.966 |
| 0.02 | 4358.832 | 35.51127 | 126.8748 | 1787.649 | 2152.069 |
| 0.03 | 4357.894 | 35.47051 | 126.9108 | 1786.520 | 2152.533 |
| 0.04 | 4354.302 | 35.44665 | 126.9296 | 1783.198 | 2152.089 |
| 0.05 | 4355.549 | 35.46102 | 126.9633 | 1784.077 | 2152.338 |

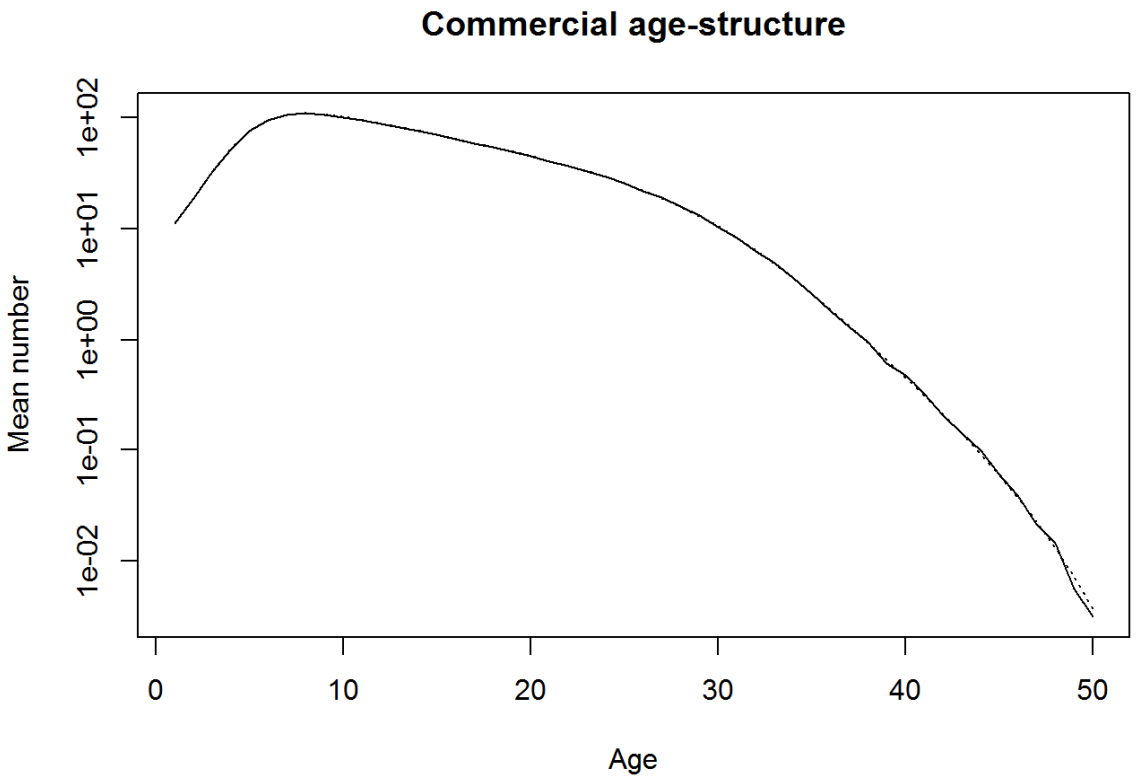


Fig 18. Mean of the expected commercial catches-at-age high MSYR fit of model (dashed line) compared with the true mean catch-at-age (solid line) from Test scenario 3.


Fig 19. Mean of the special permit expected catches-at-age from high MSYR fit of model (dashed line) compared with the true mean catch-at-age (solid line) from Test scenario 3

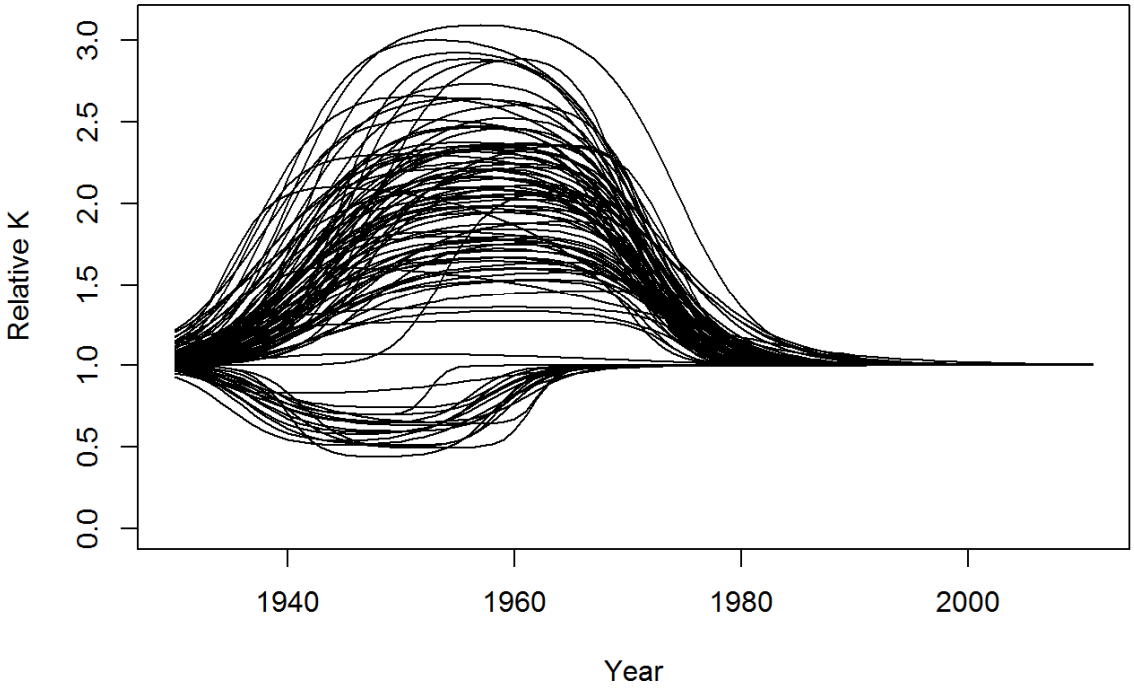


Fig 20. The trends in *K* from high MSYR fit of model for Test Scenario 3.

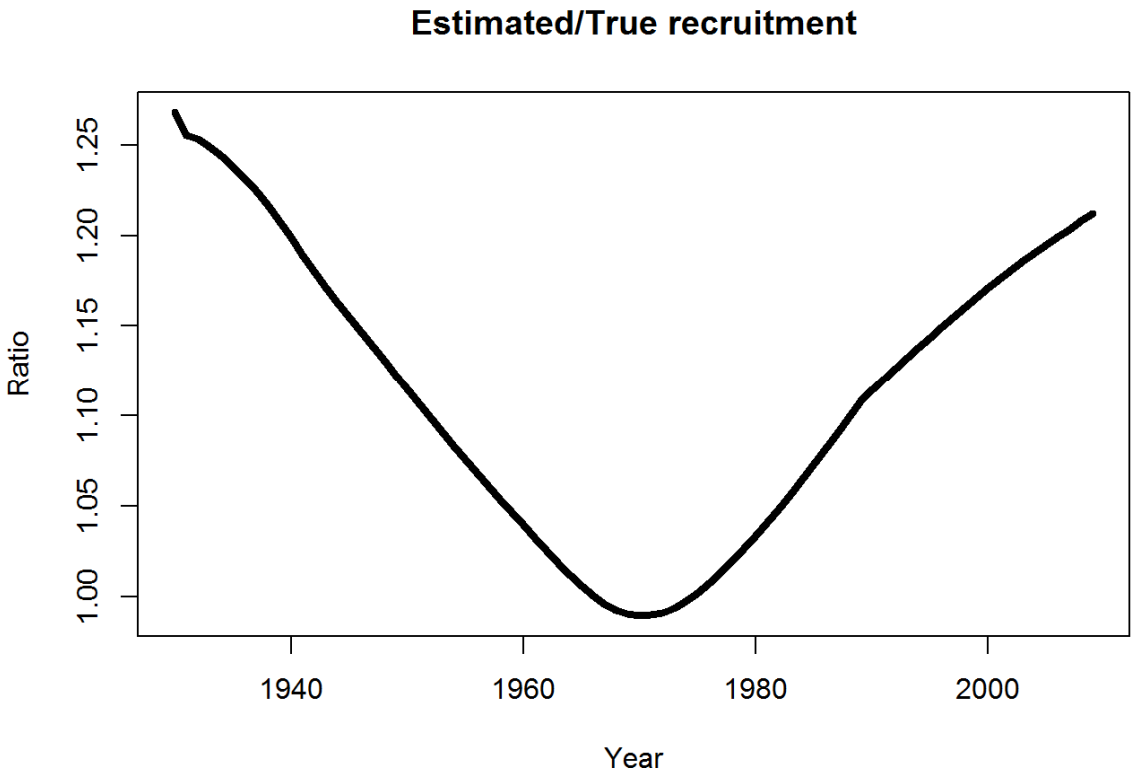


Fig 21. The estimated bias in recruitment from high MSYR fit of model under Test Scenario 3.

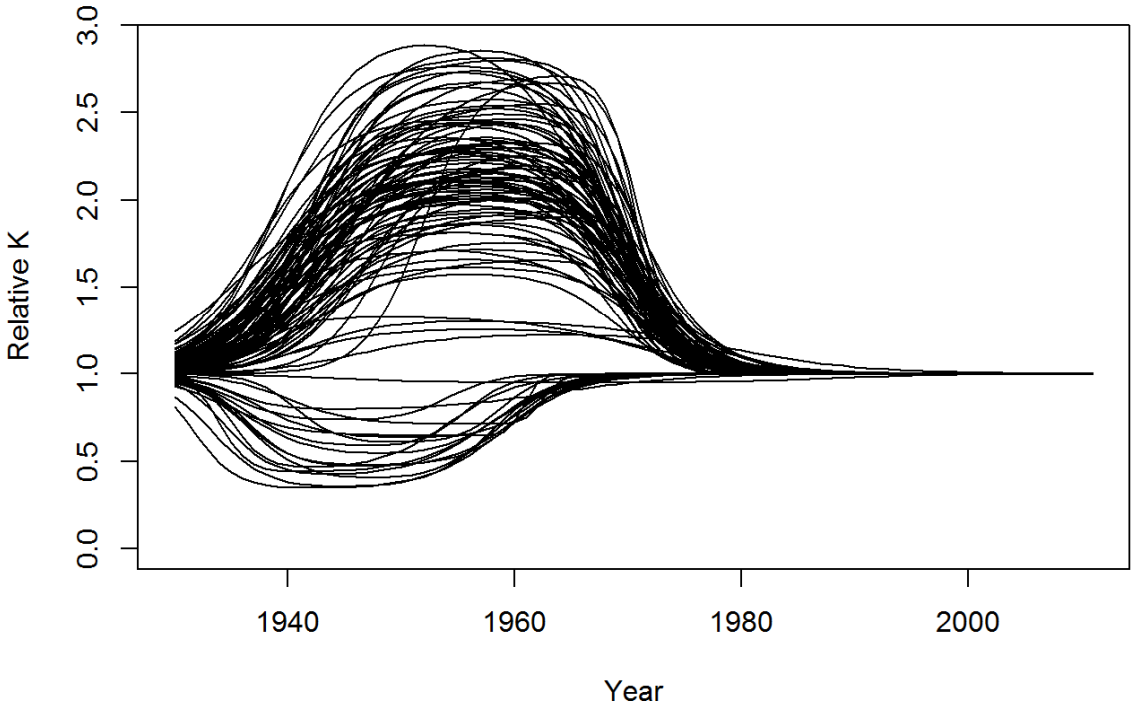


Fig 22. The trends in *K* from low MSYR fit of model for Test Scenario 3.

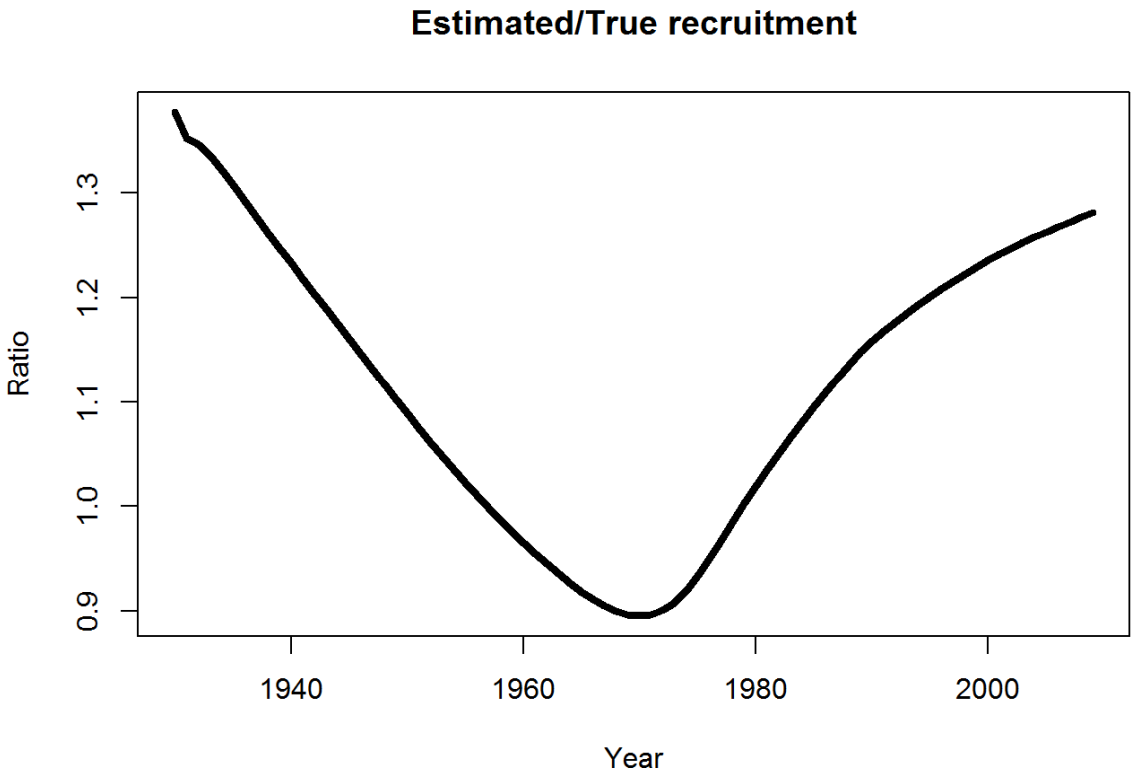


Fig 23. The estimated bias in recruitment from low MSYR fit of model under Test Scenario 3.

**Test 4 *K* increases and then declines with variability = 0.3 – density dependence is 75% in natural mortality and 25% in births**

This scenario includes the random variability in $K = 0.3$ and thus these results can be compared with Test scenario 1. Table 5 shows that the estimates of MSYR have roughly the same statistics as for Tests 1, 2 and 3, with similar bias dependency on the starting values and similar coefficients of variation. The estimates for delta *K* are biased lower than in Test 3 and consequently even more biased compared with Test 1. Figs 24 and 27 show that a substantial proportion of the estimates of delta *K* are negative, which leads to substantial downward bias in the estimates and consequently greater CVs. Figs 25 and 26 show a time varying bias of 25 to 35% at similar levels to Test 3. In this case recruitment multipliers are estimated. The recruitment multipliers in Figs 26 and 29 show similar trends to the Test 1 case (Figs 8 and 11), but in this scenario the magnitudes of the mean multipliers are generally closer to unity, which is where they should be. The marginal likelihoods in Table 5 for delta *K* and MSYR now suggest that there is no virtually no information about MSYR or delta *K* in the range tested.

*Table 5. Properties of estimates from Test 4. The first sub-table are the estimates of MSYR and Delta K from 100 trials. The second sub-table is the mean marginal total negative log-likelihood profiles from 25 trials with identical data for fixed values of Delta K, and also subdivided for the different data sources. The third sub-table is the mean marginal total negative log-likelihood profiles from 25 trials with identical data for fixed values of MSYR, and also subdivided for the different data sources.*

| Start | MSYR estimates (true = 0.0364) | | | | Delta *K* estimates (true = 2.0) | | | |
|---|---|---|---|---|---|---|---|---|
| | Mean | SD | CV | Bias | Mean | SD | CV | Bias |
| High | 0.046 | 0.0099 | 0.218 | 1.250 | 0.40 | 0.734 | 0.199 | 1.179 |
| Low | 0.018 | 0.0052 | 0.293 | 0.489 | 0.30 | 0.491 | 1.653 | 0.149 |

| Delta K | Total | Survey 1 | Survey 2 | Comm. Ages | S. permit Ages |
|---|---|---|---|---|---|
| 0.0 | 4322.475 | 35.24713 | 126.0430 | 1765.808 | 2140.228 |
| 1.0 | 4322.008 | 35.21260 | 125.8410 | 1765.774 | 2140.406 |
| 2.0 | 4323.116 | 35.23657 | 125.9003 | 1767.099 | 2139.898 |
| 3.0 | 4323.027 | 35.14972 | 125.6036 | 1767.761 | 2140.135 |
| 4.0 | 4322.623 | 35.29910 | 125.9246 | 1765.826 | 2140.471 |

| MSYR | Total | Survey 1 | Survey 2 | Comm. Ages | S. permit Ages |
|---|---|---|---|---|---|
| 0.01 | 4321.992 | 35.22781 | 125.9430 | 1765.510 | 2140.313 |
| 0.02 | 4322.058 | 35.21850 | 125.9030 | 1765.648 | 2140.356 |
| 0.03 | 4322.178 | 35.20571 | 125.8400 | 1765.823 | 2140.495 |
| 0.04 | 4322.337 | 35.21456 | 125.8978 | 1765.749 | 2140.586 |
| 0.05 | 4322.125 | 35.19206 | 125.9052 | 1765.646 | 2140.578 |

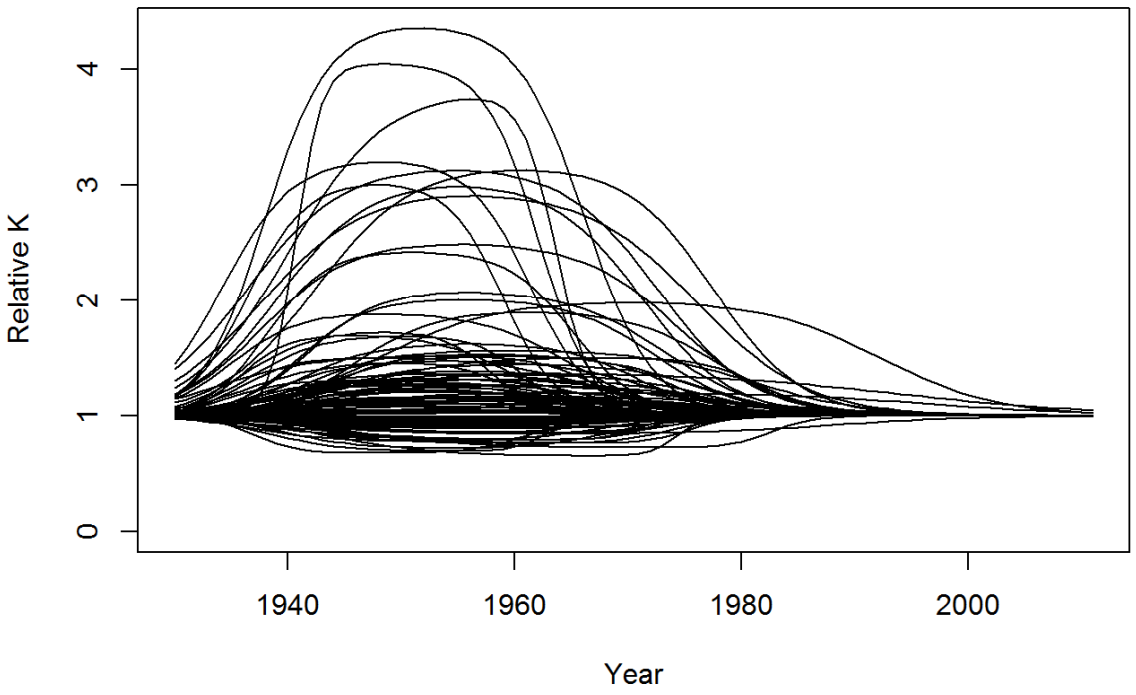


Fig 24. The trends in *K* from high MSYR fit of model for Test Scenario 4.

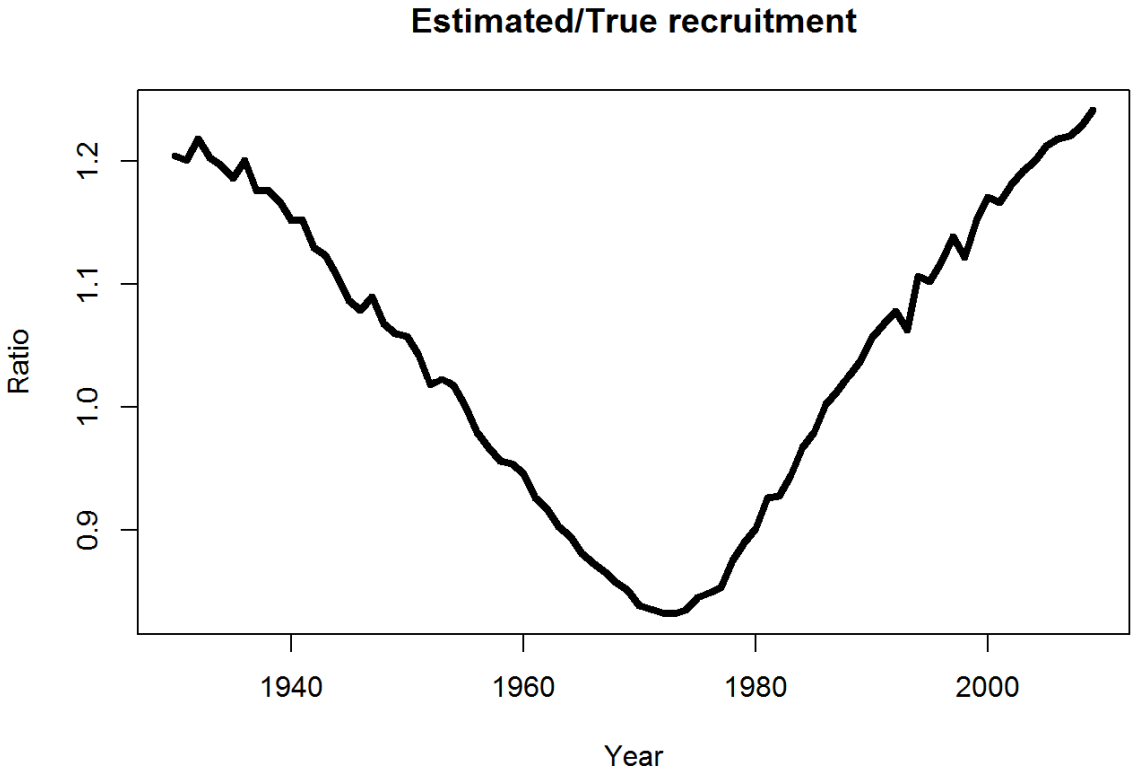


Fig 25. The estimated bias in recruitment from high MSYR fit of model under Test Scenario 4.

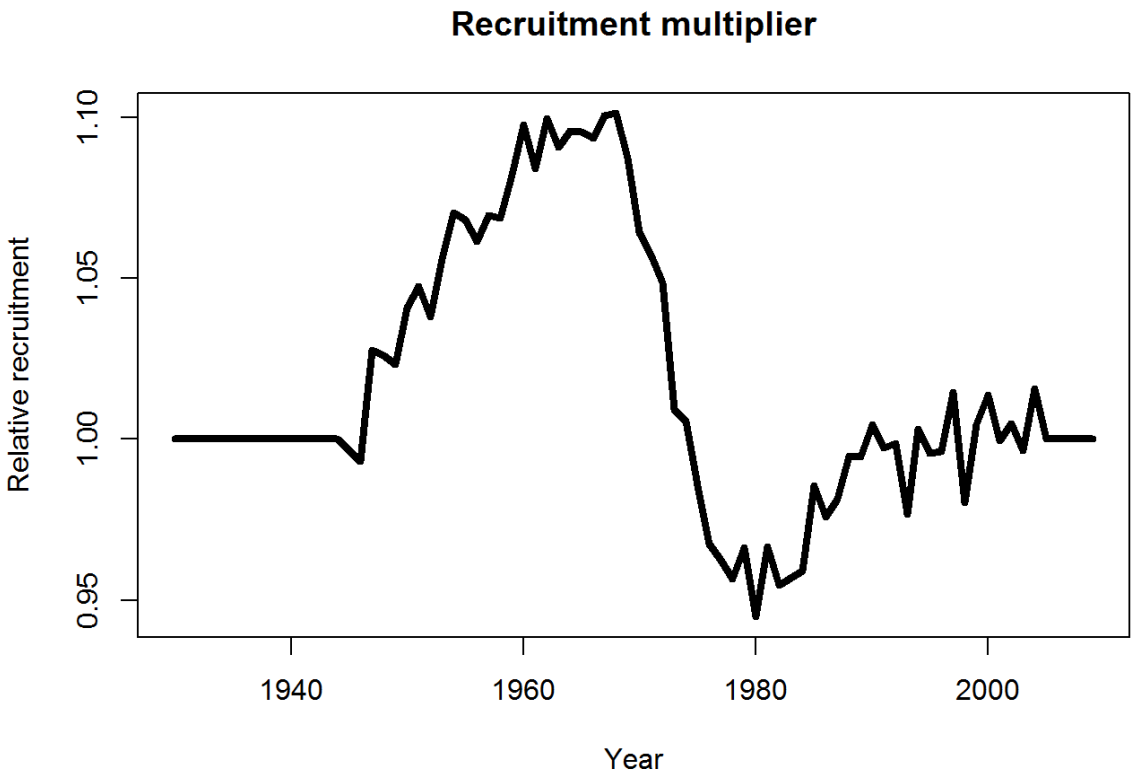


Fig 26. The means of the recruitment multiplier estimates from high MSYR fit of model under Test scenario 4.

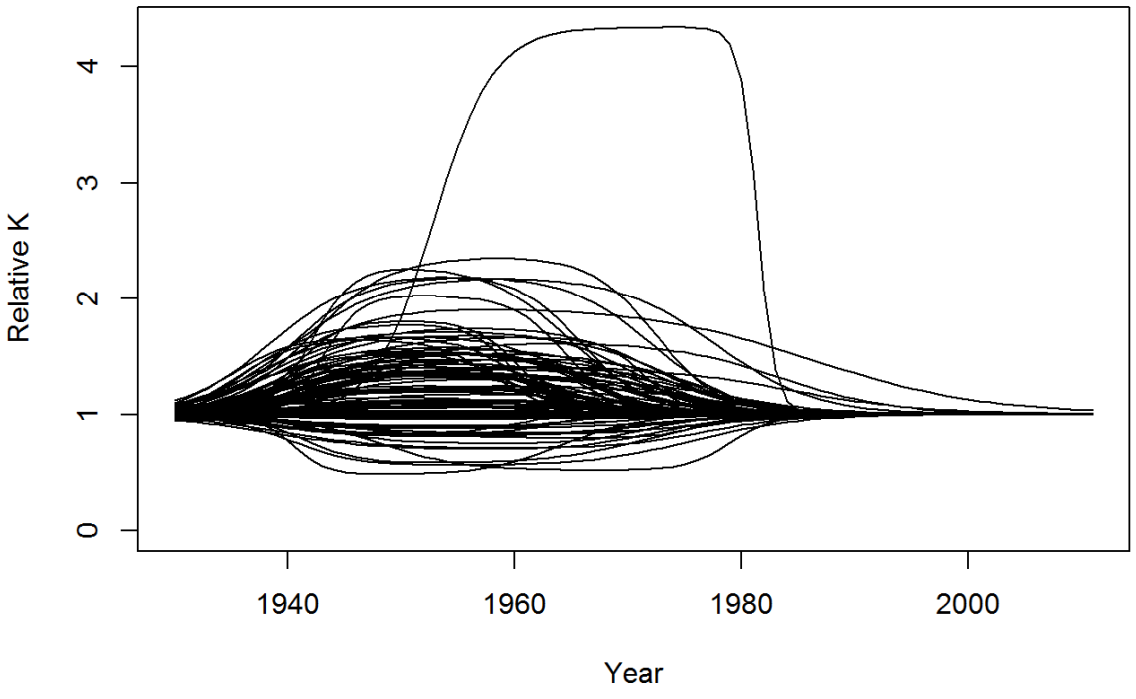


Fig 27. The mean estimated recruitment trajectory (dashed line) from the low MSYR fit of model compared with mean trajectory for Test scenario 4.

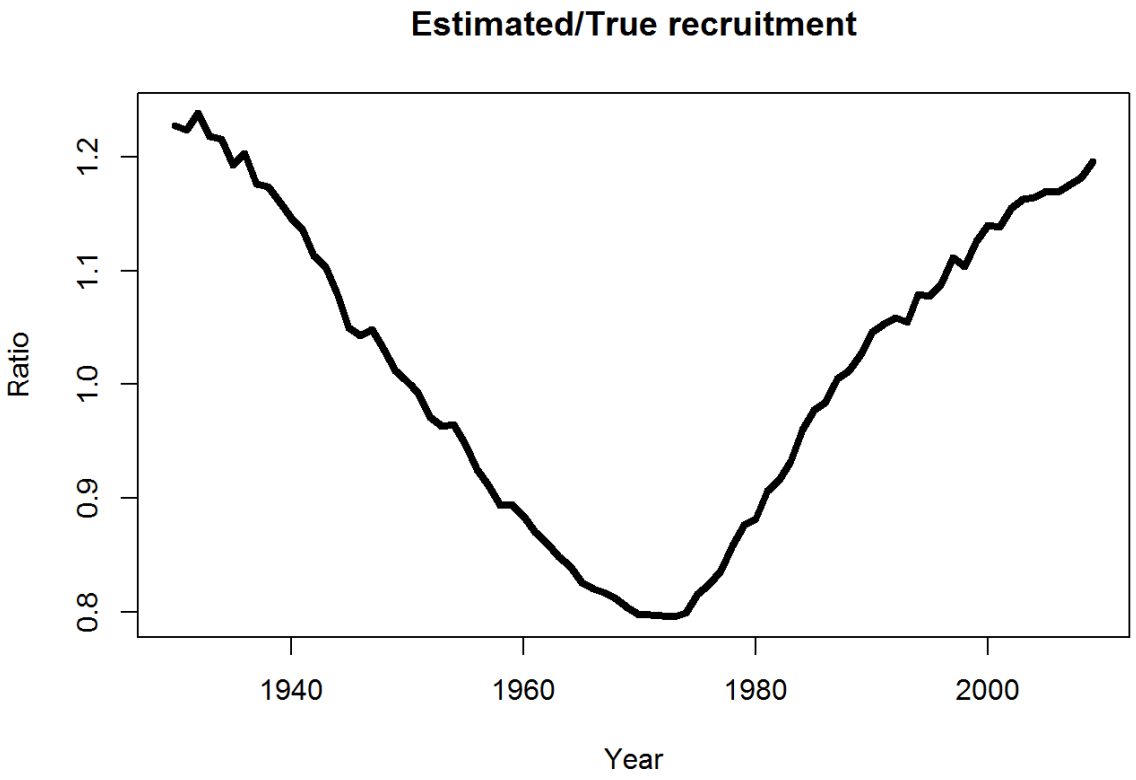


Fig 28. The estimated bias in recruitment from low MSYR fit of model under Test Scenario 4.

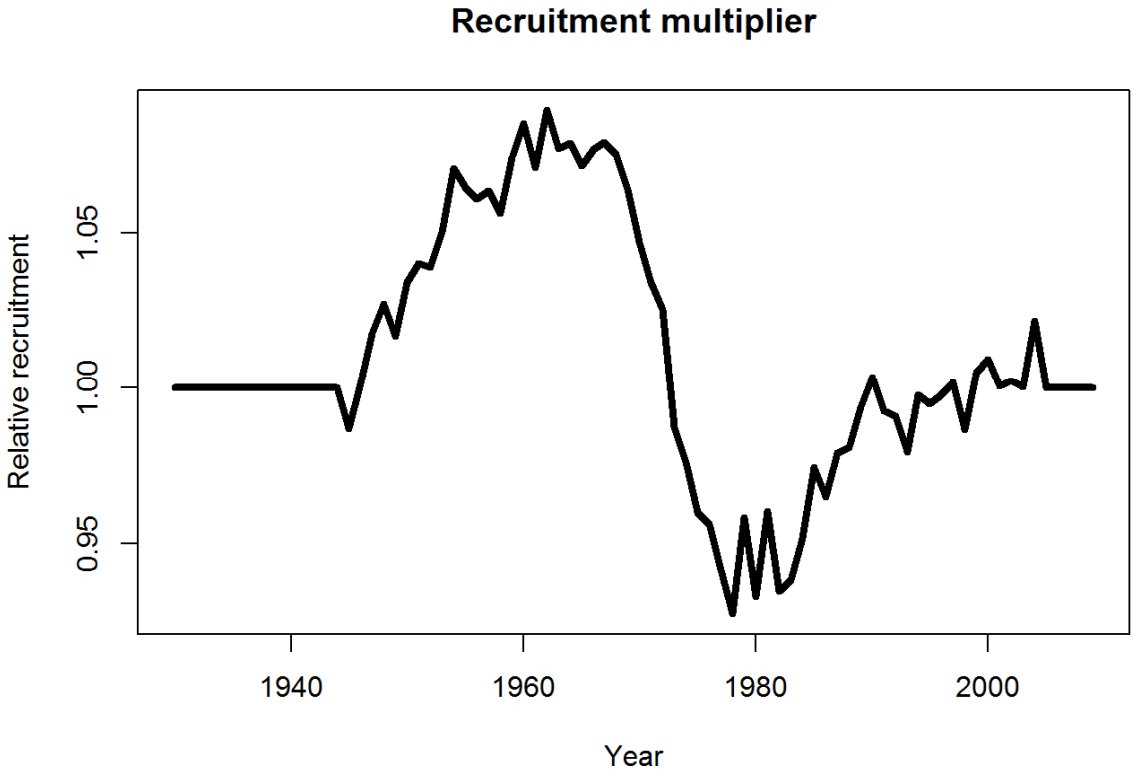


Fig 29. The means of the recruitment multiplier estimates from low MSYR fit of model under Test scenario 4.

**Test 5 No trend or variability in *K*, 75% density dependence in natural mortality 25% in births (1)**
A possible scenario for Southern hemisphere minke whales is that there has been no substantial trend in *K*. This test examines the properties of fitting the model that attempts to estimate a single increase in *K* even though it is in fact absent. The scenario assumes that no decline in *K* occurs during the period for which the data are available. Table 6 shows that the estimates of MSYR have similar properties to the previous scenarios. The mean of the estimated trends in *K* are on average reasonably close to the true value zero. The estimates of MSYR are similar to the previous scenarios with biases that depend on the start value. The marginal likelihoods in Table 6 again suggest that there is little information about MSYR. There appears to be some possibility of discriminating against erroneous large changes in *K*.

*Table 6. Properties of estimates from Test 5. The first sub-table are the estimates of MSYR and Delta K from 100 trials. The second sub-table is the mean marginal total negative log-likelihood profiles from 25 replicates with identical data for each fixed value of Delta K, and also subdivided for the different data sources. The third sub-table is the mean marginal total negative log-likelihood profiles from 25 replicates with identical data for each fixed value of MSYR, and also subdivided for the different data sources.*

| Start | MSYR estimates (true = 0.0364) | | | | Delta *K* estimates (true = 2.0) | | | |
|---|---|---|---|---|---|---|---|---|
| | Mean | SD | CV | Bias | Mean | SD | CV | Bias |
| High | 0.050 | 0.0070 | 0.140 | 1.358 | -0.001 | 0.119 | - | - |
| Low | 0.018 | 0.0036 | 0.199 | 0.492 | 0.0443 | 0.184 | 4.144 | - |

| Delta K | Total | Survey 1 | Survey 2 | Comm. Ages | S. permit Ages |
|---|---|---|---|---|---|
| 0.0 | 4314.222 | 34.42292 | 124.1987 | 1783.714 | 2121.087 |
| 1.0 | 4310.988 | 34.47086 | 124.2342 | 1781.681 | 2119.838 |
| 2.0 | 4311.863 | 34.52216 | 124.1976 | 1782.858 | 2120.512 |
| 3.0 | 4312.852 | 34.40360 | 124.2058 | 1786.446 | 2125.290 |
| 4.0 | 4318.044 | 36.15476 | 126.8764 | 1795.228 | 2131.685 |

| MSYR | Total | Survey 1 | Survey 2 | Comm. Ages | S. permit Ages |
|---|---|---|---|---|---|
| 0.01 | 4311.999 | 34.46292 | 124.3046 | 1782.022 | 2120.156 |
| 0.02 | 4312.028 | 34.46822 | 124.2426 | 1782.087 | 2120.221 |
| 0.03 | 4311.993 | 34.46041 | 124.2288 | 1782.124 | 2120.219 |
| 0.04 | 4312.244 | 34.44576 | 124.2229 | 1782.830 | 2120.360 |
| 0.05 | 4312.239 | 34.46099 | 124.2082 | 1782.279 | 2120.349 |

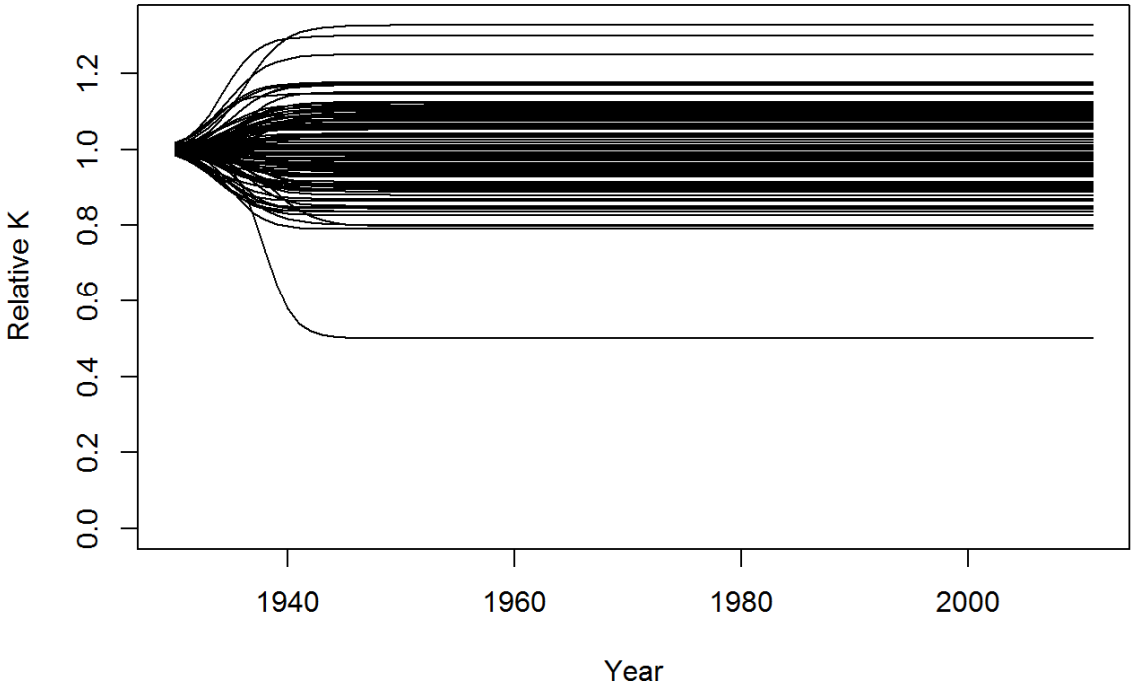


Fig 30. The trends in *K* from high MSYR fit of model for Test Scenario 5.

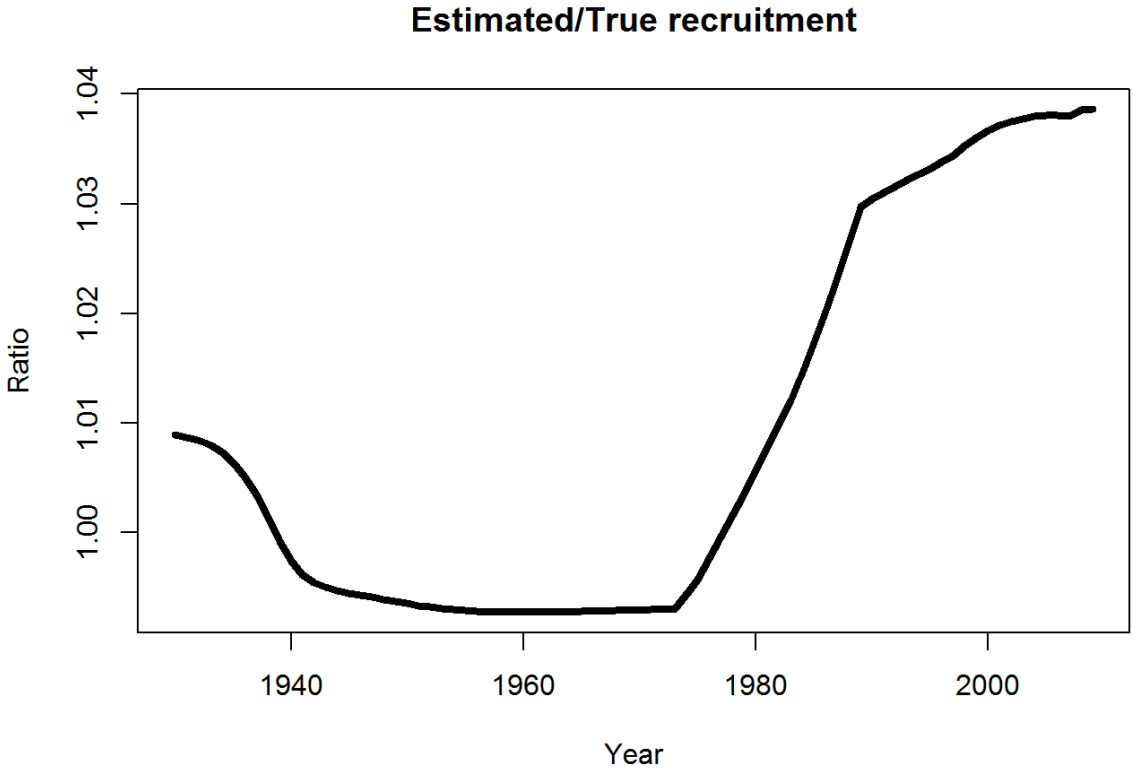


Fig 31. The estimated bias in recruitment from high MSYR fit of model under Test Scenario 5.

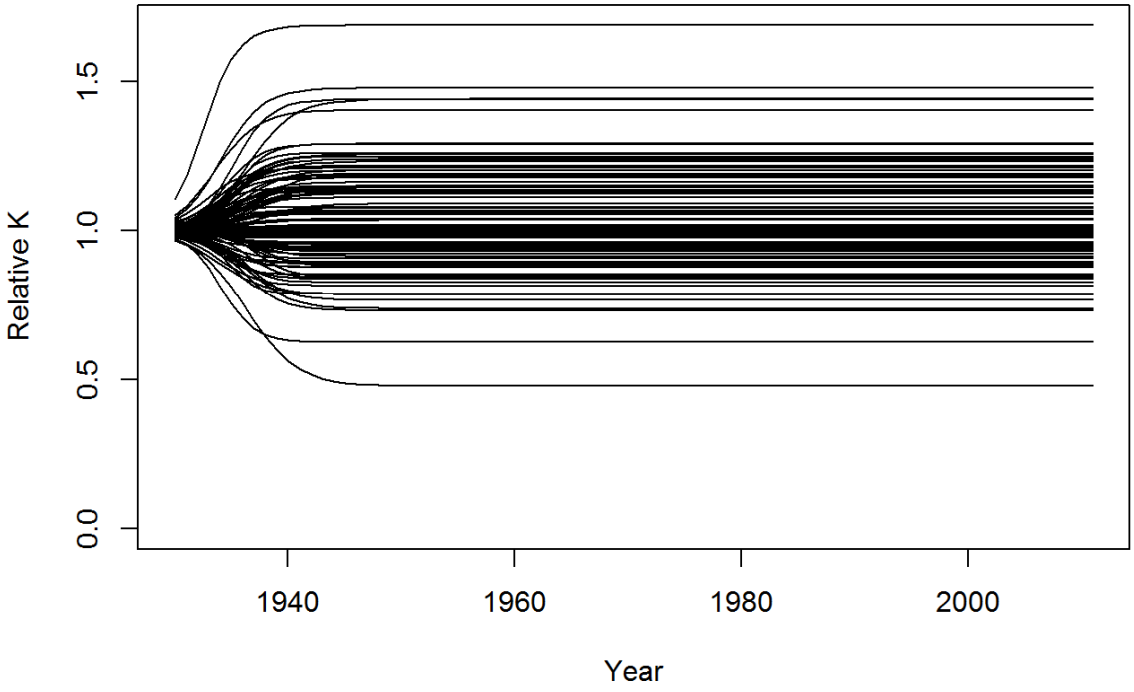


Fig 32. The trends in *K* from low MSYR fit of model for Test Scenario 5.

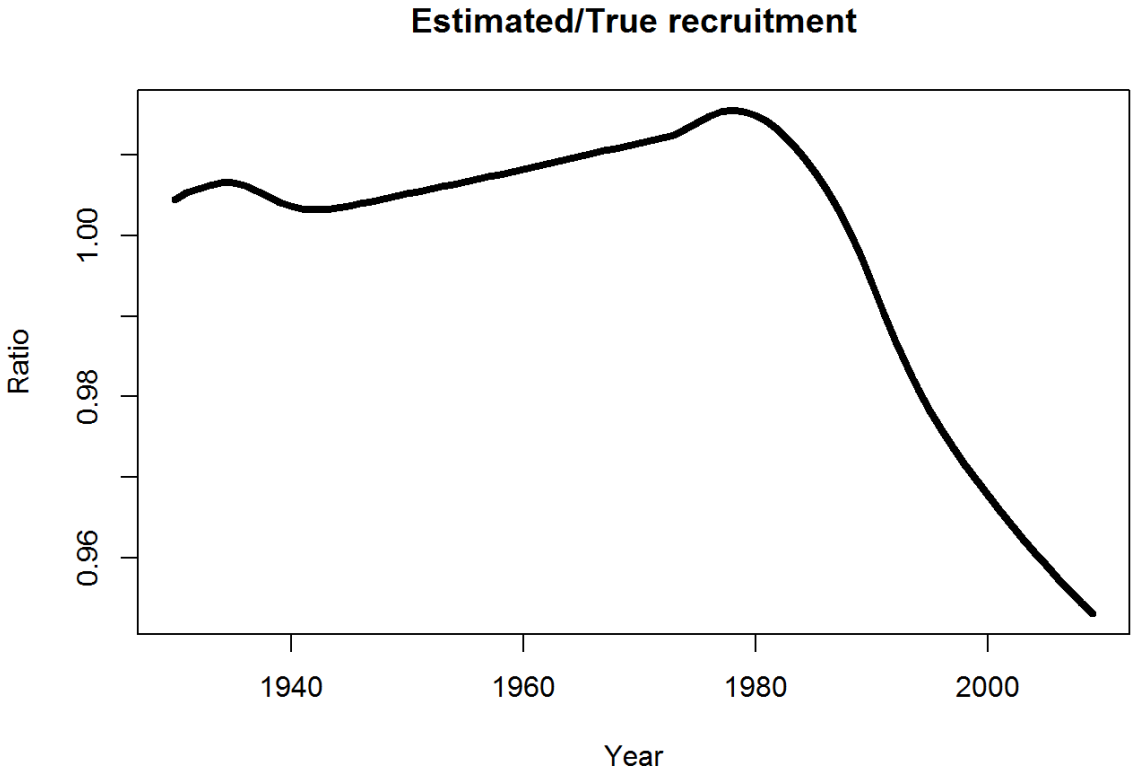


Fig 33. The estimated bias in recruitment from low MSYR fit of model under Test Scenario 5.

**Test 6 *K* increases during the 1930s with delta *K* = 2 and remains constant thereafter**
Another plausible scenario for Southern hemisphere minke whales is that there has been a trend in *K* beginning in the 1930s and given that some whale stocks remain depleted that *K* will remain high for some years to come. This test examines the properties of fitting the model that attempts to estimate a single increase in *K* and assumes that no decline in *K* occurs during the period for which the data are available. Table 7 shows that the estimates of MSYR have similar properties to the previous scenarios. The mean of the estimated trends in *K* are substantially below their true value of two. The marginal likelihoods in Table 7 again suggest that there is little information about MSYR or delta *K*. Estimated trends in recruitment bias shown in (Figs 35 and 37) show that the estimates of recruitment trends are unreliable.

*Table 7. Properties of estimates from Test 6. The first sub-table are the estimates of MSYR and Delta K from 100 trials. The second sub-table is the mean marginal total negative log-likelihood profiles from 25 replicates with identical data for each fixed value of Delta K, and also subdivided for the different data sources. The third sub-table is the mean marginal total negative log-likelihood profiles from 25 replicates with identical data for each fixed value of MSYR, and also subdivided for the different data sources.*

| Start | MSYR estimates (true = 0.0364) | | | | Delta *K* estimates (true = 2.0) | | | |
|---|---|---|---|---|---|---|---|---|
| | Mean | SD | CV | Bias | Mean | SD | CV | Bias |
| High | 0.049 | 0.0115 | 0.235 | 1.345 | 0.0860 | 0.235 | 2.731 | 0.043 |
| Low | 0.025 | 0.0142 | 0.578 | 0.672 | 0.1079 | 0.284 | 2.632 | 0.054 |

| Delta K | Total | Survey 1 | Survey 2 | Comm. Ages | S. permit Ages |
|---|---|---|---|---|---|
| 0.0 | 4328.034 | 37.63392 | 136.4373 | 1774.898 | 2106.374 |
| 1.0 | 4328.171 | 37.72100 | 136.4184 | 1774.633 | 2106.505 |
| 2.0 | 4327.287 | 37.65029 | 136.4207 | 1774.457 | 2106.655 |
| 3.0 | 4327.133 | 37.63953 | 136.3484 | 1773.927 | 2106.614 |
| 4.0 | 4328.010 | 37.53304 | 136.1609 | 1774.156 | 2108.049 |

| MSYR | Total | Survey 1 | Survey 2 | Comm. Ages | S. permit Ages |
|---|---|---|---|---|---|
| 0.01 | 4327.125 | 37.66591 | 136.4815 | 1773.955 | 2106.260 |
| 0.02 | 4327.451 | 37.66359 | 136.4614 | 1774.226 | 2106.356 |
| 0.03 | 4327.541 | 37.65710 | 136.4498 | 1774.287 | 2106.378 |
| 0.04 | 4327.620 | 37.65046 | 136.4349 | 1774.390 | 2106.512 |
| 0.05 | 4327.789 | 37.65149 | 136.4335 | 1774.608 | 2106.436 |

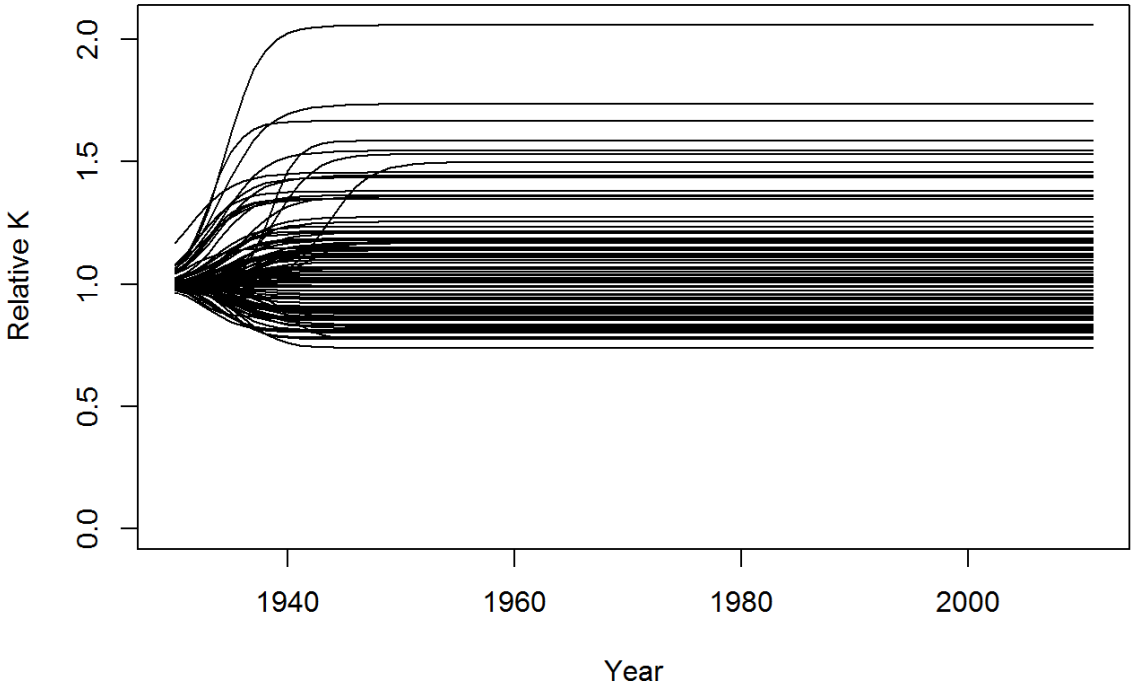


Fig 34. The trends in *K* from high MSYR fit of model for Test Scenario 6.

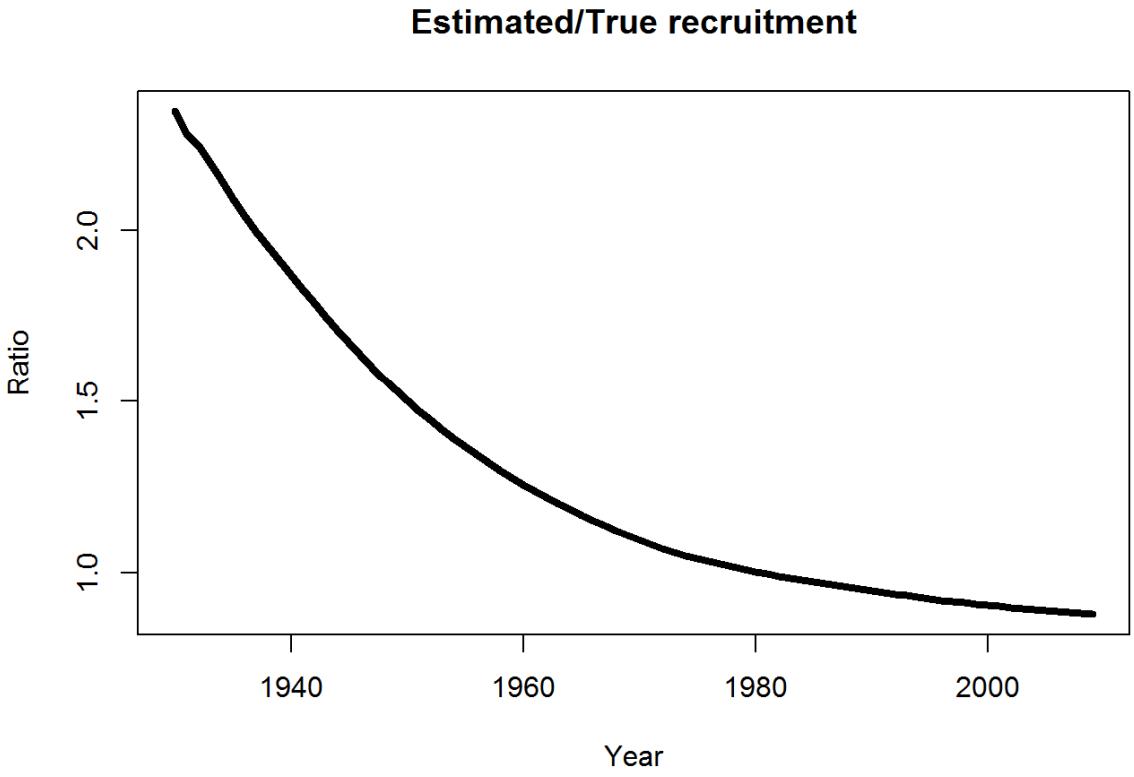


Fig 35. The estimated bias in recruitment from high MSYR fit of model under Test Scenario 6.

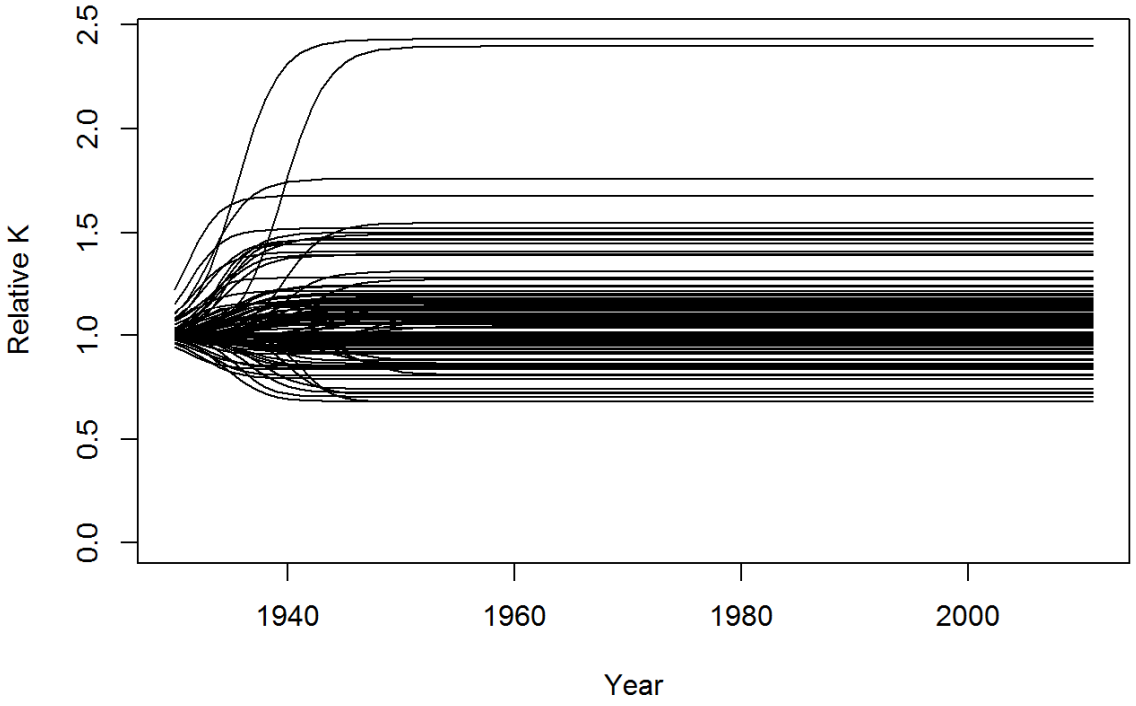


Fig 36. The trends in *K* from low MSYR fit of model for Test Scenario 6.

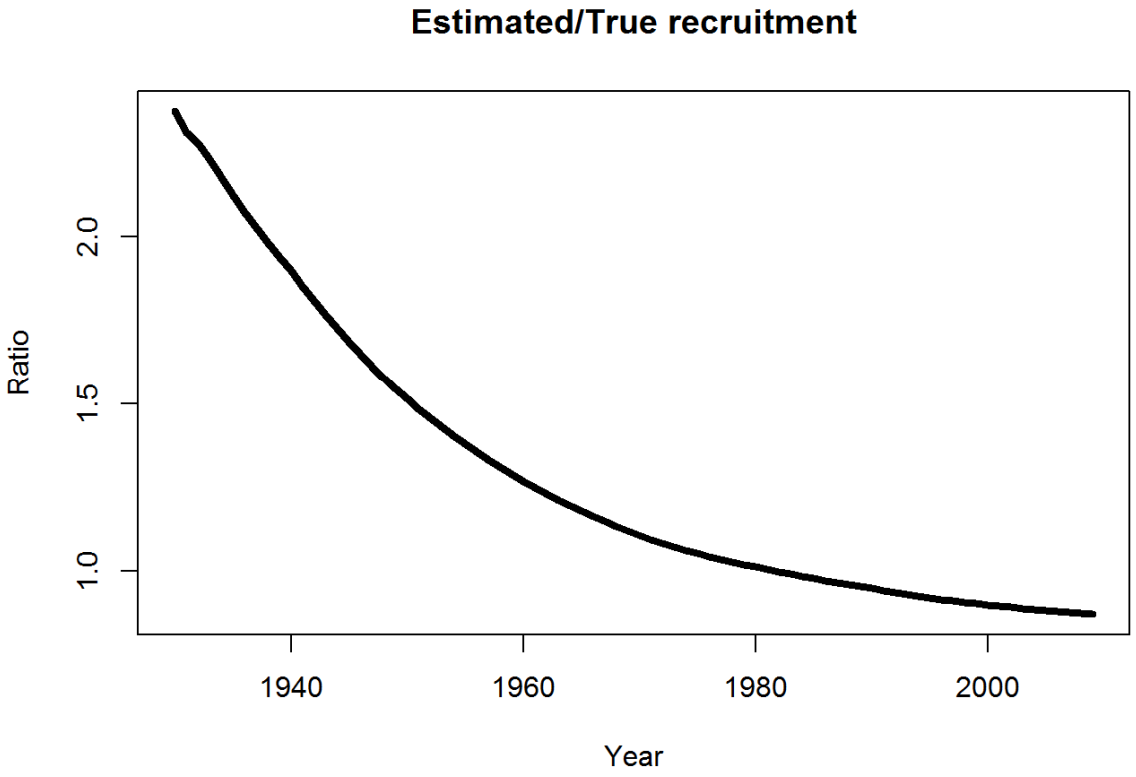


Fig 37. The estimated bias in recruitment from low MSYR fit of model under Test Scenario 6.

**Test 7 *K* increases during the 1930s with delta *K* = 2 but the fitted model allows for both an increase and decrease in *K***

This scenario for Southern hemisphere minke whales is the same as the preceding one that there has been a trend in *K* beginning in the 1930s and that *K* will remain high for some years to come. This test examines the properties of fitting the model that allows for *K* to change in both directions during the period for which the data are available, i.e. similar to the other models where trends in *K* are estimated using a dome shaped function. Table 8 shows that the estimates of MSYR have similar properties to the previous scenarios. Figs 38 and 40 show that a dome shaped function is fitted to the data even though there is no downward trend in *K*. The mean of the estimated values of delta *K* are substantially below their true value of two. The marginal likelihoods in Table 8 again suggest that there is little information about MSYR or delta *K*. Estimated trends in recruitment bias shown in (Figs 39 and 41) show that the estimates of recruitment trends are unreliable.

*Table 8. Properties of estimates from Test 7. The first sub-table are the estimates of MSYR and Delta K from 100 trials. The second sub-table is the mean marginal total negative log-likelihood profiles from 25 trials with identical data for fixed values of Delta K, and also subdivided for the different data sources. The third sub-table is the mean marginal total negative log-likelihood profiles from 25 trials with identical data for fixed values of MSYR, and also subdivided for the different data sources.*

| Start | MSYR estimates (true = 0.0364) | | | | Delta *K* estimates (true = 2.0) | | | |
|---|---|---|---|---|---|---|---|---|
| | Mean | SD | CV | Bias | Mean | SD | CV | Bias |
| High | 0.051 | 0.0100 | 0.195 | 1.405 | -0.008 | 0.477 | - | -0.004 |
| Low | 0.025 | 0.0142 | 0.578 | 0.672 | 0.1079 | 0.284 | 2.632 | 0.054 |

| Delta K | Total | Survey 1 | Survey 2 | Comm. Ages | S. permit Ages |
|---|---|---|---|---|---|
| 0.0 | 4322.243 | 37.58487 | 135.8363 | 1774.10 | 2102.805 |
| 1.0 | 4322.117 | 37.60627 | 135.9541 | 1774.12 | 2102.504 |
| 2.0 | 4322.652 | 37.62167 | 135.9796 | 1774.45 | 2102.620 |
| 3.0 | 4323.325 | 37.64382 | 135.7619 | 1775.44 | 2103.164 |
| 4.0 | 4322.538 | 37.69553 | 136.0076 | 1775.08 | 2101.973 |

| MSYR | Total | Survey 1 | Survey 2 | Comm. Ages | S. permit Ages |
|---|---|---|---|---|---|
| 0.01 | 4322.511 | 37.59491 | 135.8737 | 1773.86 | 2103.219 |
| 0.02 | 4322.686 | 37.58510 | 135.8621 | 1773.96 | 2103.347 |
| 0.03 | 4322.146 | 37.55094 | 135.8218 | 1773.67 | 2103.275 |
| 0.04 | 4321.756 | 37.57662 | 135.7887 | 1773.59 | 2102.929 |
| 0.05 | 4321.617 | 37.56715 | 135.7940 | 1773.52 | 2102.923 |

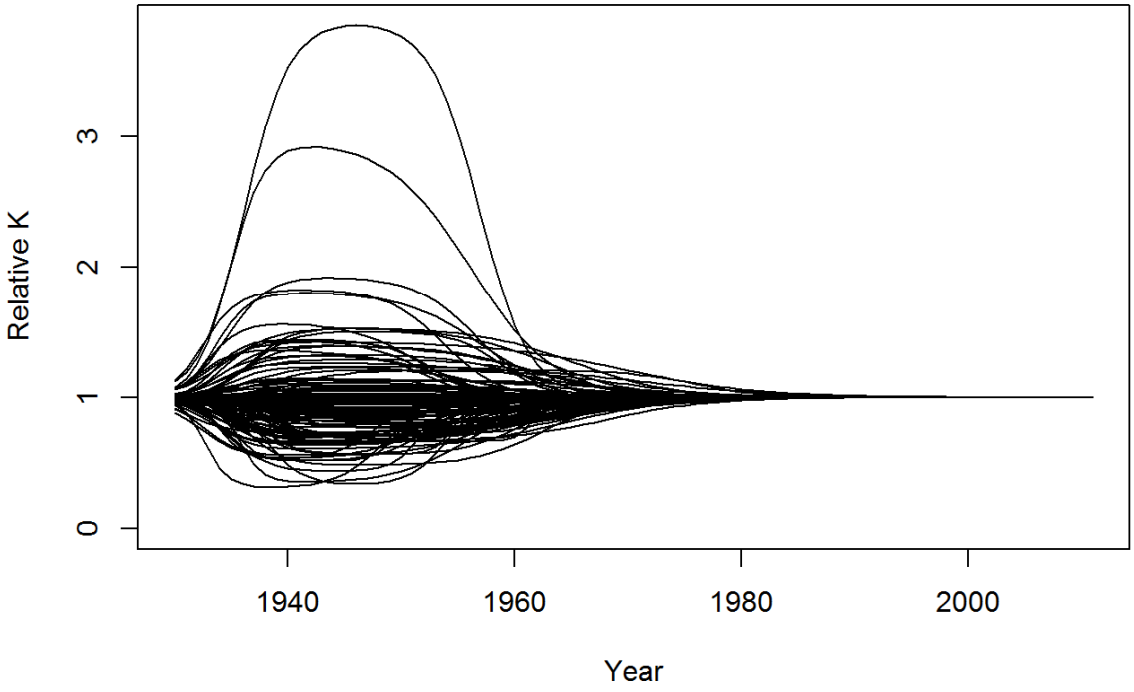


Fig 38. The trends in *K* from high MSYR fit of model for Test Scenario 7.

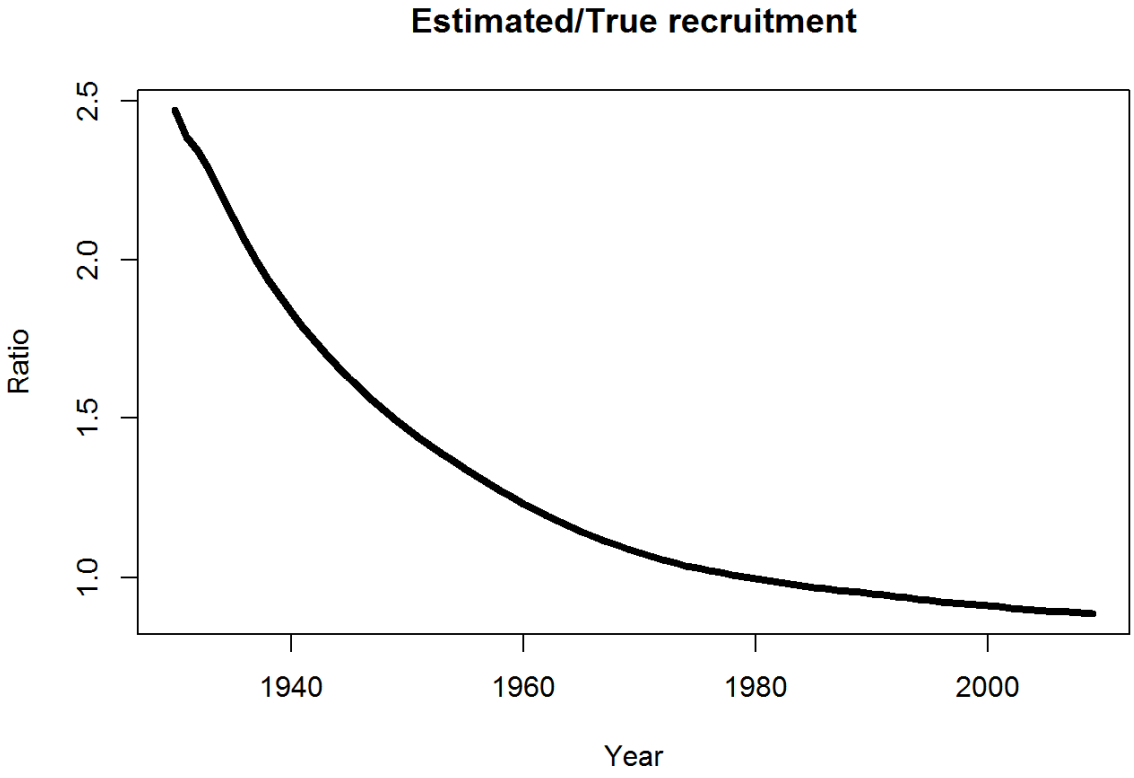


Fig 39. The estimated bias in recruitment from high MSYR fit of model under Test Scenario 7.

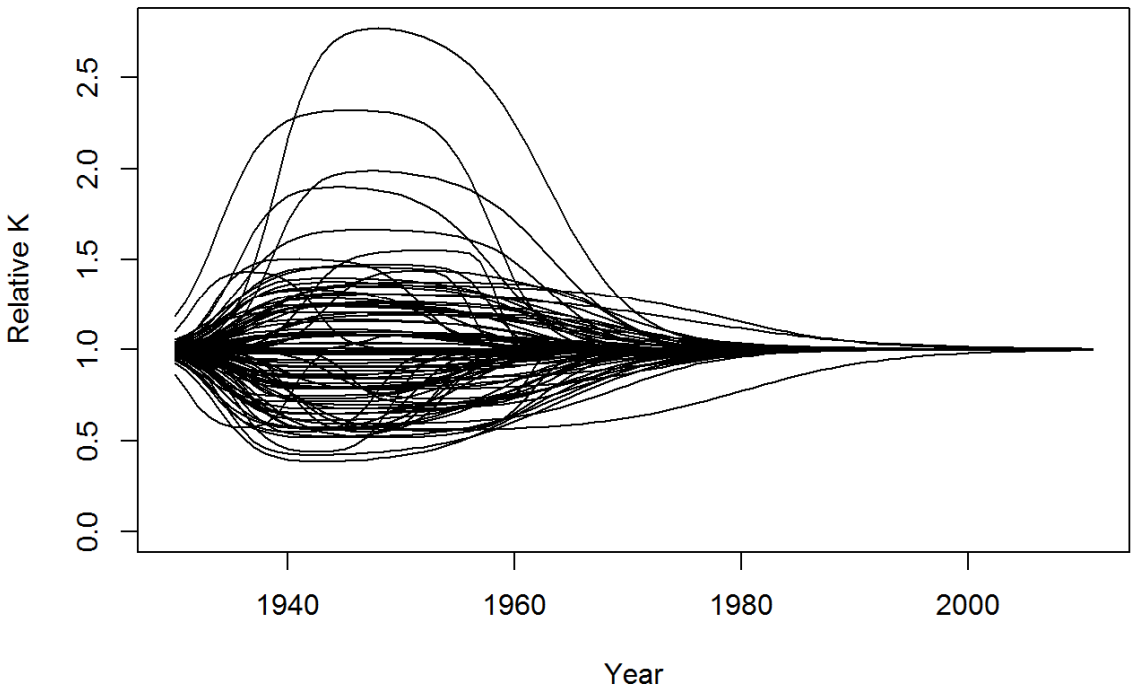


Fig 40. The trends in *K* from low MSYR fit of model for Test Scenario 7.

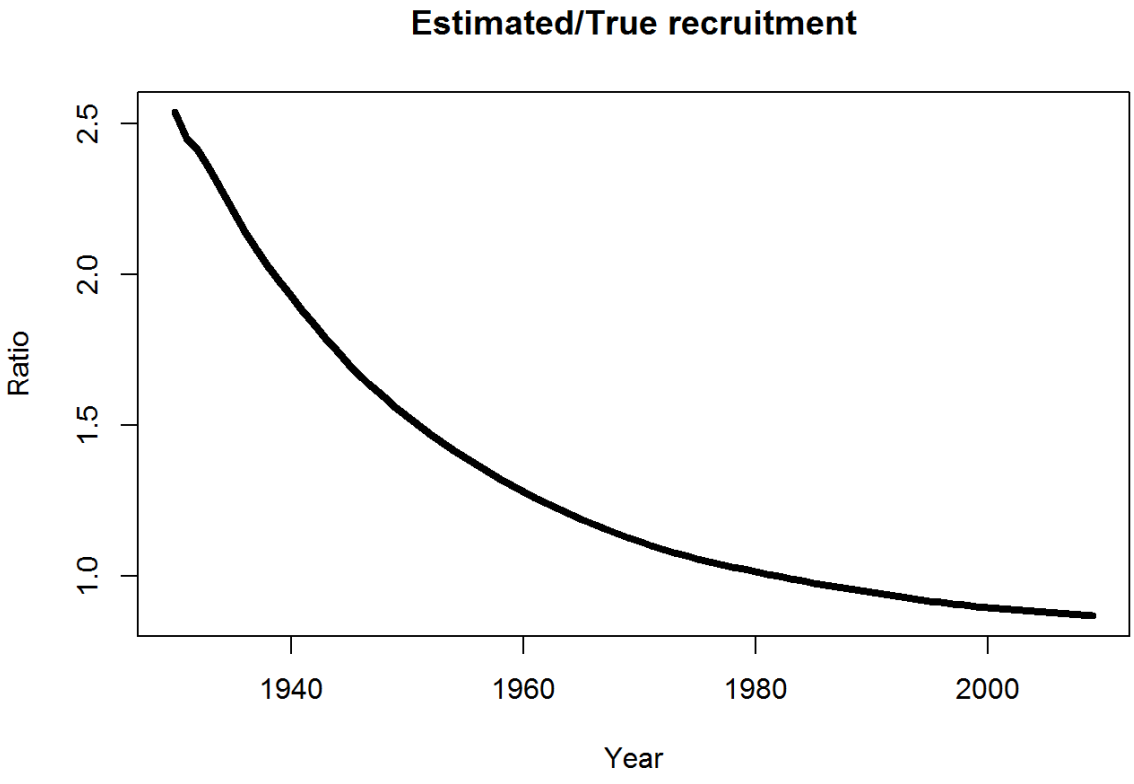


Fig 41. The estimated bias in recruitment from low MSYR fit of model under Test Scenario 7.

**Conclusion**

SCAA methods are not of course unsound in principle, however, reliable results depend on choosing an appropriate form of model to fit to the data. The existing SCAA can be improved by using (continuous)

functions with parameters that can be estimated for describing trends in *K*, natural mortality, recruitment and selectivity.

The poor properties of the estimates demonstrated here arise primarily from the amount and type of data not being sufficient. In particular the historical data is where the contrast in stock size occurs that makes if feasible in principle to estimate some of the parameters of interest. However, the test reported here suggest that the historical contrast is relatively uninformative given the amount of data available. The more recent and future data are from a period when even less contrast exists or can be expected in relation to population changes. For this reason the recent data are not informative about trends in *K* or MSYR and the collection of further data has little effect on improving precision of such estimates. Moreover the estimation of trends in recruitment are subject to biases that are sensitive to both model formulation and assumptions about suitable starting points for the estimation of MSYR.

These trials show that interpreting the results of SCAA models may not be straightforward. The sensitivity of the estimates of MSYR to the starting values used in the search is a property of the search algorithm. When the data are uninformative for a given parameter the derivative of the objective function with respect to that parameter is zero (or very close to it). This means that the search algorithm will not shift that parameter by any appreciable amount during the search because it is in effect already at the minimum. Thus the final value tends to be anchored to the start value. The variability shown in the results is probably the result of the dithering applied when selecting the start values for each replicate, and hence not a proper reflection of the uncertainty of the parameter estimate. A similar effect is probably driving the estimated decline in *K* in Test 7 where no such decline should be estimated. If Bayesian methods were to be applied, the posterior distribution of the parameters for which there was little or no information would be little changed from the prior distribution, which is a potential diagnostic for this issue. Similarly distributions of parameters derived from Monte Carlo Markov Chain methods may be adversely affected if the selected proposal distribution does not properly reflect the lack of information for some of the parameters.

## References

de la Mare, W. K and Miller, E. 2016. Further examination of the relationship between MSYR1+ and MSYR mature based on individual based energetic models. (This meeting).

Logan, G. de la Mare, W., King, J. and Haggarty, D. 2005. *Management framework for Strait of Georgia Lingcod*. Research Document 2005/048, Canadian Science Advisory Secretariat, Department of Fisheries and Oceans Canada, Ottawa. 116 pp.

Press, W. H., Teukolsky, S. A., Vetterling, W. T. and Flannery, B. P. 1992. Numerical recipes in C++: the art of scientific computing. Cambridge University Press. 963pp.

Punt, A.E. 2011. Further analyses related to the application of statistical catch-at-age analysis to Southern Hemisphere minke whales. Paper SC/63/IA1 presented to the IWC Scientific Committee, May 2011 (unpublished). 20pp.Punt, A.E. and T. Polacheck. 2005. Application of statistical catch-at-age analysis for Southern Hemisphere minke whales in Antarctic Areas IV and V. Document SC/57/IA9 presented to the IWC Scientific Committee, June 2005. (unpublished). 71pp.

Punt, A. E., Bando, T., Hakamada, T. and Kishiro, T. 2014. Assessment of Antarctic Minke Whales using Statistical Catch-at-age Analysis. SC/65/IA01. Presented to the IWC Scientific Committee, June 2014.

Punt, A.E. and T. Polacheck. 2006. Further statistical catch-at-age analyses for Southern Hemisphere minke whales. Document SC/57/IA2 presented to the IWC Scientific Committee, June 2006. (unpublished). 40pp.

Punt, A.E. and T. Polacheck. 2007. Further development of statistical catch-at-age models for Southern Hemisphere minke whales. Document SC/59/IA4 presented to the IWC Scientific Committee, May 2007. (unpublished). 42pp.

Punt, A.E. and Polacheck, T. 2008. Further analyses related to the application of statistical catch-at-age analysis to Southern Hemisphere minke whales. Paper SC/60/IA2 presented to the IWC Scientific Committee, June 2008 (unpublished). 46pp.Punt

Siler, W. 1979. A competing-risk model for animal mortality. Ecology 60:750-757.

## APPENDIX A: POPULATION DYNAMICS MODEL

### Age-Structured Dynamics

The dynamics model an age-structured model derived from a class library written in C++. A list of the parameters used in the model is given in Table E.1. The basic dynamic equations are given by:

$$N_{a+1,t+1} = \left(N_{a,t} - C_{a,t}\right) S_{a,t} \qquad \left|0 \le a < \left(a_{\max} - 1\right)\right. \tag{A.1}$$

with:

$N_{a,t}$ number in age class $a$ in year $t$,

$C_{a,t}$ catch in number from age class $a$ in year $t$,

$S_{a,t}$ proportion of fish that survive after natural mortality from age $a$ to $a$+1 in year t

$$S_{a,t} = \mathrm{e}^{-M_{a,t}} \tag{A.2}$$

with:

$M_{a,t}$ natural mortality rate at age $a$ in year $t$. Natural mortality is age dependent and denoted as depending and time because it can be specified as being density dependent. The age-dependence is given by a modified Siler age-dependent mortality function (an extra parameter is used to defer the onset of higher mortality for the older age classes):

$$M_{a,t} = \beta_1 \exp\left(-\beta_2 a\right) + \beta_{3,t} + \beta_4 \exp\left(a - \beta_5\right) \tag{A.3}$$

Density dependence in natural mortality arises from:

$$\beta_{3,t} = \beta_{3,K} + \left(\beta_{3,0} - \beta_{3,K}\right)\left(1 - \left(\frac{B_t}{K}\right)^z\right) \tag{A.4}$$

where:

| | |
|---|---|
| $\beta_{3,t}$ | natural mortality at stock biomass $B_t$, |
| $\beta_{3,K}$ | natural mortality at carrying capacity $K$ |
| $\beta_{3,0}$ | natural mortality at negligible stock size |
| $B_t$ | biomass in year t |
| $K$ | biomass at carrying capacity |
| $Z$ | density dependent exponent |

There is a pooled age class (plus class) at $a = a_{\max}$ . For this class:

$$N_{a_{\max},t+1} = \left(N_{a_{\max},t} - C_{a_{\max},t}\right) S_{a_{\max},t} + \left(N_{a_{\max}-1,t} - C_{a_{\max}-1,t}\right) S_{a_{\max}-1,t} \tag{A.5}$$

Catch-at-age by operation $j$ in year $t$ is estimated (and fitted to observed catch-at-age) using:

$$C_{j,a,t} = H_{j,t} s_{j,a} N_{a,t} \tag{A.6}$$

with:

$s_{j,a}$ age-specific selectivity for operation $j$, i.e. the proportion of age class a vulnerable to the fishery.

$H_{j,t}$ is the proportional harvest rate of operation $j$ in year $t$, specifically:

$$H_{j,t} = \frac{C_{j,t}}{\sum_{a=0}^{a_{\max}} N_{a,t} s_{j,a}} \tag{A.7}$$

with:

$C_{j,t}$ total catch in number by operation $j$ over all ages in year $t$

The model is coded so that time can be advanced in arbitrary increments, including zero. Catches can be removed at any time step and at as many time steps as required. Different catch series can be removed from the population at the same time step, or at different times if required. In the current application the time step used is one year.

The age-specific selectivity can be specified arbitrarily. In this current application two parametric forms of selectivity are applied, either a logistic function, or a 'dome' shape derived from the product of two logistic functions. The logistic function is given by:

$$s_{j,a} = \frac{1}{1 + e^{-g_j\left(a - a_{j,s50}\right)}} \tag{A.8}$$

with:

$a_{\bullet,s_{50}}$ age at which 50% of a cohort is vulnerable to fishing from operation *j*, and

$g_j$ a constant which determines the rate at which selectivity changes with age. Specifically:

$$g_j = \frac{\ln(19)}{\left(a_{j,s_{95}} - a_{j,s_{50}}\right)} \tag{A.9}$$

with:

$a_{j,s_{95}}$ age at which 95% of a cohort is vulnerable to fishing from operation *j*.

The 'dome shaped' selection function is the product of a logistic and a reverse logistic function:

$$s_{j,a} = \frac{1}{\left(1+e^{-g_j\left(a-a_{j,s50}\right)}\right)\left(1+e^{h_j\left(a-a_{j,\mu 50}\right)}\right)} \tag{A.10}$$

Masses at age are calculated using a growth curve and a mass length relationship, that is:

$$w_{a,t} = AL_{a,t}{}^{B} + 0.5 \cdot AB(B-1)L_{a,t}{}^{B-2}\,\mathrm{V}[L_{a,t}] \tag{A.11}$$

with:

constants A and B

$L_{a,t}$ length at age from the growth curve. This can depend on *t* because the growth curve can be specified to be density dependent

$\mathrm{V}[L_{a,t}]$ variance of length at age *a* in year *t*.

It is assumed that $\mathrm{V}[L_{a,t}]$ is well approximated by $\left(L_{\bullet,a,t}\xi_L\right)^2$, where $\xi_L$ is a constant coefficient of variation applicable to the variability of length at age for all ages. Consequently:

$$w_{\bullet,a,t} = AL_{\bullet,a,t}{}^{B}\left(1+0.5 \cdot B(B-1)\xi_L{}^2\right) \tag{A.12}$$

The second terms in equations E.9 and E.10 are a "delta method" corrections required because an animal of mean length (i.e. from a growth curve) is not an animal whose mass is equal to the mean mass at age. However, in this application, in accordance with the common practice, $\mathrm{V}[L_{a,t}]$ is assumed to be zero.

Length at age is given by a von Bertalanffy growth curve:

$$L_a = L_\infty\left(1-\mathrm{e}^{-k(a-a_0)}\right) \tag{A.13}$$

with:

$L_\infty$ asymptotic mean length at age

$k$ rate constant

$a_0$ intercept

The proportion of animals sexually mature at each age is given by an ogive

$$m_a = \frac{1}{1+e^{-\mu\left(a-a_{\mu_{50}}\right)}} \tag{A.14}$$

with:

$a_{\mu_{50}}$ age at which 50% of a cohort is mature and

$\mu$ a constant which determines the rate at which maturity changes with age. Specifically:

$$\mu = \frac{\ln(19)}{\left(a_{\mu_{95}} - a_{\mu_{50}}\right)} \tag{A.15}$$

with:

$a_{j,s_{95}}$ age at which 95% of a cohort is vulnerable to fishing from operation *j*.

**Stock Recruitment Relationships**

***Logistic stock-recruit relationship***

The number of recruits into age-class zero in year *t* is given by:

$$N_{0,t} = \frac{B_t\alpha}{1+\exp(\beta(B_t - B_{50}))} \tag{A.16}$$

Where $B_t$ is the mature female component of the population and $B_{50}$ is the inflexion point of the reversed logistic. This model thus has density dependence in fecundity depending on mature biomass. Approximate yield curve due to changes in recruitment (given recruits per mature female at *K* ( $\rho_K$ )) is given by:

$$y = B\left(\frac{\alpha}{1+\exp\left(\beta\left(B-B_{50}\right)\right)}-\rho_K\right) \tag{A.17}$$

$B_{\mathrm{MSYL}}$ is the solution to the following equation:

$$\frac{dy}{dB}=\frac{\alpha}{D}-\frac{\alpha\beta B\left(D-1\right)}{D^2}-\rho_K=0 \tag{A.18}$$

where

$$D=1+\exp(\beta(B-B_{50})) \tag{A.19}$$

MSYR is close to directly proportional to alpha, which is effectively proportional to the recruits per mature female at negligible stock size. MSYL is determined by the value of beta, which can be determined by finding the root of (equation 0.4) with *B* fixed at MSYL. Thus the SRR is fully described by the two parameters $\alpha$ and $\beta$. If *K* is to be varied by a multiple (during minimisation), say $K'=\xi K$ then $\beta'=\frac{\beta}{\xi}$. This preserves MSYR, and MSYL retains the same value as a proportion of $K'$. Given the values of alpha and beta, B50 is given by:

$$B_{50}=K-\frac{\log\left(\frac{\alpha}{\rho_K}-1\right)}{\beta} \tag{A.20}$$

This SRR has the advantage that MSYL can take a wide range of values, similarly to the Pella-Tomlinson, but with the further advantage that recruitment does not become negative at stock sizes somewhat above *K*. This is an advantage when fitting models using auto-differentiation because there are no negative recruitments that need to be set to zero, which thus avoids discontinuous derivatives that disrupt the minimisation algorithm.
The model can be specified with a choice of three other commonly used stock recruitment relationships (SRRs); Beverton and Holt, Ricker and Pella-Tomlinson. An additional SRR is available that allows depensation in the Beverton and Holt model. In this application only the logistic form is used. Fig A1 shows two examples of yield curves from the logistic SRR. These are very similar to the shapes of the corresponding yield curves from a Pella-Tomlinson model.

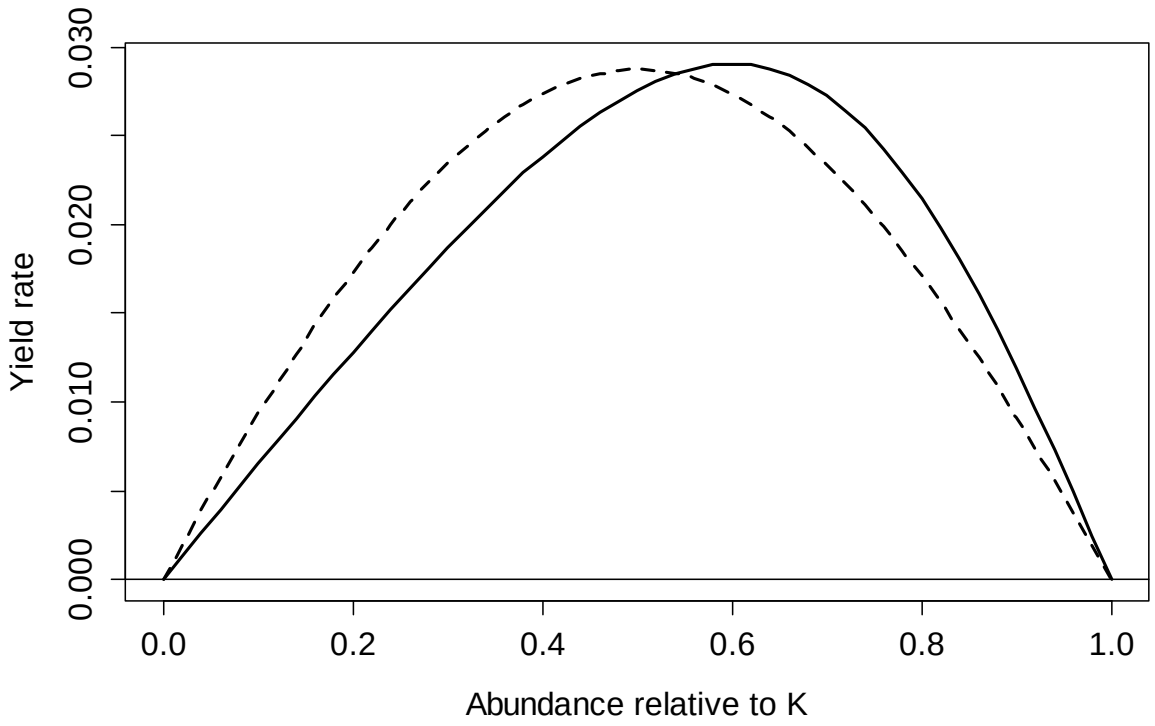


Fig A1. Two yield curves from the logistic model, with MSYLs of 0.5 and 0.6.

**Variability in recruitment**
When required, the effects of recruitment variability can be included by multiplying the numbers of recruits by a random lognormal number ρ with an expected value of 1.0 and a specified coefficient of variation (ξR). The same random multiplier is used for both males and females at the same age, so that the total recruitment is

variable but the sex ratio at each age is not. Recruitment variability can also be driven by multiplying Kt by a random number from log-normal distribution.

**Fitting the Model to Data**

The first data to be fitted is the total catch. Although in principle the catches could be taken as given and simply removed from the population, it is helpful instead to estimate an annual exploitation rate (as a proportion of the vulnerable population). This helps in the minimisation because for some trial values of population size some age-classes will go extinct, which leads to discontinuous derivatives and the failure of the search algorithm. The total catch in a given year is given by:

$$\hat{C}_t = \sum_j \sum_{a=1}^{a_{\max}} \hat{h}_{j,t} \hat{s}_{j,a} \hat{N}_{a,t} \tag{A.21}$$

Where $\hat{h}_{j,t}$ is the estimated exploitation rate in year *t* for operation (fleet) *j*. These are essentially a nuisance parameters. The observed catches are assumed to have a log normal distribution with a very small, constant CV so that in the final estimates the differences between the observed and expected total catches are small. This portion of the overall likelihood function is given by:

$$-\mathrm{L}\left(\boldsymbol{\Theta}\middle|\mathbf{C}\right) = n\left(\ln\left(\sigma_C\right) + \ln\left(\sqrt{2\pi}\right)\right) + \frac{1}{2}\frac{\sum_{C_t>0}\left(\ln\left(C_t\right) - \ln\left(\hat{C}_t\right) + \frac{1}{2}\sigma_C^2\right)^2}{\sigma_{C_t}^2} \tag{A.22}$$

Where n is the number of non-zero catches, $\sigma_c$ is a small number essentially the artificial coefficient of variation of the observed catch $C_t$. The other terms represent an additive constant, which could normally be ignored, but they are included here so that the relative contributions to the total likelihood have appropriate magnitudes. This is the same method as used in the existing SCAA. Fig 1 shows that the catches are estimated using this function with negligible error.

The variants of the model are fitted to the time series of surveys using a log-likelihood function based on the assumption that the survey estimates have log-normal distributions with an estimated coefficient of variation. The log-likelihood is given by:

$$-\mathrm{L}(\boldsymbol{\Theta}|\mathbf{x}) = -\sum_{i=1}^{n}\ln\left(x_i\right) - \frac{n}{2}\ln\left(2\pi\right) - \sum_{i=1}^{n}\ln\left(\sigma_i\right) - \frac{1}{2}\sum_{i=1}^{n}\left(\frac{\ln\left(x_i\right) + \frac{1}{2}\sigma_i{}^2 - \ln\left(\mathrm{E}\left[x_i\right]\right)}{\sigma_i}\right)^2 \tag{A.23}$$

where:

| | |
|---|---|
| n | number of surveys in the series |
| $x_i$ | is the *i*th survey estimate |
| $\sigma_i$ | estimated standard deviation of the log-transformed survey estimate |

and $\mathrm{E}\left[x_i\right] = q_j \hat{N}_i$ where $q_j$ is the survey bias correction for survey series *j* and $\hat{N}_t$ is the modelled abundance of the 1+ population in the corresponding survey year *t*.

The fitting to the catch-at-age data assumes that the data have multinomial distributions, with Log-likelihood given by:

$$-\mathrm{L}\left(\boldsymbol{\Theta}\middle|\mathbf{n}\right) = -\ln N! + \sum_{i=1}^{k+1}\ln n_a! - \sum_{i=1}^{k+1} n_a \ln p_a \tag{A.24}$$

Where **n** is a vector of catches at age in a given year, *N* is the total sample size of catch-at-age in that year, $n_a$ is catch in age-class *a* and $p_a$ is the modelled probability of catching an animal at that age as determined by the modelled age-structure in the given year and the relevant selectivity function.

The parameter vector $\boldsymbol{\Theta}$, is estimated by minimising the sum over the various data types of the negative log likelihood functions using a conjugate gradient method (*frpmin* from the numerical recipes library, Press et al 1992.) using derivatives calculated by auto-differentiation.